GFZ
POTSDAM

Originally published as:

Wolf, D., Klemann, V., Wünsch, J., Zhang, F.-P. (2006): A Reanalysis and Reinterpretation of Geodetic and Geological Evidence of Glacial-Isostatic Adjustment in the Churchill Region, Hudson Bay. - Surveys in Geophysics, 27, 1, 19-61,

DOI: 10.1007/s10712-005-0641-x.

A reanalysis and reinterpretation of geodetic and geological evidence of glacial-isostatic adjustment in the Churchill region, Hudson Bay

Detlef Wolf, Volker Klemann, Johann Wünsch and Fei-peng Zhang
GeoForschungsZentrum Potsdam, Telegrafenberg, 14473 Potsdam, Germany

September 1, 2004

Abstract. We review the historical, geological, tide-gauge, GPS and gravimetric evidence advanced in favour of, or against, continuing land uplift around Hudson Bay, Canada. We also reanalyse the tide-gauge and GPS data for Churchill using longer time series than those available to previous investigators. The dependence of the mean rate of relative sea-level change obtained from the tide-gauge record on the length and mid-epoch of the observation interval considered is investigated by means of a newly developed linear-trend analysis diagram. For studying the shorter-period variability of the tide-gauge record, the wavelet transform is used. The mean rate of land uplift obtained from GPS is based on a new analysis using IGS solutions of GFZ. To include the post-glacial land uplift, sea-level indicators from the Churchill region representing the relative sea-level history during the past 8000 a are also included. Finally, the values of the four observables are jointly inverted in terms of mantle viscosity. The optimum values are $\sim 3.2 \times 10^{20}$ Pa s and $\sim 1.6 \times 10^{22}$ Pa s for the upper- and lower-mantle viscosities, respectively.

Keywords: Absolute gravimetry, glacial-isostatic adjustment, GPS, linear-trend analysis, mantle viscosity, sea-level indicator, tide gauge, wavelet-transform analysis

1. Introduction

The present-day as well as post- and late-glacial changes of the level of the sea or the height of the land can be measured using a variety of observational techniques. Apart from geological methods based on geomorphologic or organic indicators of the former sea level, several geodetic methods have been introduced to measure the present-day


© 2005 *Kluwer Academic Publishers. Printed in the Netherlands.*

changes. Most prominent among them are tide-gauge measurements, which record the relative motion between land and sea, GPS measurements, which determine the topographic-height changes of the land, and absolute-gravimetry measurements, which provide an indirect measure of the disequilibrium causing these changes.

In the formerly glaciated regions of the northern hemisphere, several fundamental geodetic stations have been established, which allow us to record the ongoing adjustment of the viscoelastic earth to the last deglaciation using several types of measurement. Among them is Metsähovi, Finland, where GPS, VLBI and absolute gravimetry – supplemented by the nearby tide gauge at Helsinki – can be used (Virtanen, 2004). The same combination of observational techniques exists at Ny-Ålesund, Svalbard, and was used to study effects due to the last deglaciation and recent ice-mass changes (Hagedoorn and Wolf, 2003). In North America, tide-gauge, GPS and absolute-gravimetry measurements are available for Churchill, Canada, and were analyzed in terms of glacial isostasy (Tushingham, 1992).

In the following, we will first review the historical and geological evidence advanced in favour of or against present-day land uplift in the Hudson Bay region (Sec. 2). Subsequently, we discuss previous analyses of the Churchill tide-gauge record and present a new analysis using a time series from 1940–2001 (Sec. 3). This is followed by a review of previous analyses of absolute-gravimetry and GPS measurements at Churchill and a new GPS analysis based on a time series from 1996–2003 (Sec. 4). Additionally, we give an overview of previous studies of the history of late- and post-glacial sea level in the Hudson Bay region and compile the indicators of former sea level from the Churchill region used in this study (Sec. 5). Finally, we review estimates of the mantle viscosity based on the late- and post-glacial sea-level history around

Hudson Bay proposed by other investigators and present a new estimate based on a joint inversion of the complete geological and geodetic data base available for the Churchill region (Sec. 6). We conclude with a brief summary of the main results achieved by our study (Sec. 7).

2. Historical and geological evidence of present-day land uplift

The first suggestion that the land around Hudson Bay continues to rise is probably due to Robert Bell (1841–1917). In several official reports of the Geological Survey of Canada published between 1875 and 1886, he described the various evidence supporting his hypothesis. Most of his 'proofs' were later compiled in Bell (1896). In this publication, he noted that, since the establishment of the posts of the Hudson's Bay Company ∼1700 in the mouths of several rivers entering into the bay, it had become increasingly difficult to reach the posts from the sea. An example is Little Whale River near Richmond Gulf, which had to be abandoned as a harbour. Of interest to Bell was in particular the situation in Sloops Cove near Churchill, where larger ships wintered during the 18th century and which had become difficult to reach even for row boats when Bell visited the cove. He also identified as important evidence partially rotten driftwood, which he had noticed along the east coast at heights of 15–25 m above the reach of the highest tides. The wood was arranged along even lines, with the material freshest at the lower altitudes and becoming progressively more decayed with increasing elevation. Bell found similar evidence in gravel terraces, which were sharp and fresh-looking, or in indications of the drying out of marshes and the advance of growth. Bell also quoted aboriginal

geographical names or historical notes suggesting a recent uplift of the land, the appearance of new islands or changes from islands to peninsulae. Furthermore, he observed beach dwellings and fish traps built from rock by the Innuit, which were found at all elevations up to ∼20 m. Summarizing the evidence, he concluded that the question of the continuation of the post-glacial land uplift around Hudson Bay could be answered in an affirmative way and suggested an uplift rate of 1.5–3 m per century and, in particular, of ∼2.1 m per century for the Churchill region.

Bell's views were challenged by Joseph Burr Tyrrell (1858–1957), who noted that the location of Fort Prince of Wales at Churchill during his visit was such that it could not have been high enough above the storm waves when constructed in 1733, if the land uplift had been ∼3.3 m since that time (Tyrrell, 1896). He also reproduced a map published in 1752 of a survey up the Churchill River ∼1746, which showed high- and low-water limits and marshy grounds as they existed more than a hundred years later. Furthermore, he reported that, on November 2, 1893, he had measured the heights of six names associated with calendar years (1741–1757, those of 1753 were also dated May 27) engraved in the rocky walls of Sloops Cove. Considering that, during winter, the cove becomes regularly filled with ice up to the level of the highest spring tide of that winter, Tyrrell concluded that the dated names (2.1 m above the level of the ice on November 2, 1893) had doubtlessly been cut while the ice in the cove had been at the peak level of the winter of 1753 (the mean break-up date is June 19). Since the ice on November 2, 1893 had been at the level of the ordinary spring tide of October 27, 1893 (Tyrrell, 1894) and, thus, ∼0.3 m lower than on May 27, 1753, this peak level would be ∼1.8 m below the names and, with a snow cover on May 27, 1753, the value could even be lower.

To Tyrrell, this indicated that the water had been about as high with respect to the names when the names were cut as it had been in 1893. This conclusion was in contrast to Bell (1896), who noted that the men might have been sitting rather than standing while cutting their names. As a further indication against continuing land uplift, Tyrrell also pointed out that the 'Furnace' – a small ship that had spent the winter of 1741/1742 in Sloops Cove – had a draft of no more than 1.8 m when lightened, but could pass the entrance to the cove only at high tide. At Tyrrell's time, the depth of the entrance was still ∼1.2 m and, furthermore, any decrease in depth of the bottom of the cove from 1.8 m to 1.2 m might also have been due to the accumulation of silt as a consequence of an artificial dam built from rock fragments at the mouth of the cove for protection. Tyrrell also noted that rings for mooring ships existed in Sloops Cove ∼1.5 m above the ice, which – although they had been doubtlessly placed there in the middle of the 18th century – were still firm and strong. Taken together, the evidence indicated to him that no significant land uplift had occurred near Churchill over a century and a half.

Johnston (1939) revisited the 'Sloops Cove problem'. He reported that, on September 26, 1934, the heights of the six names in the cove used by Tyrrell (1894; 1896) had been levelled by the Department of Railways and Canals (later Department of Transport) with reference to the low-water datum of the CHS charts and with respect to mean sea level at Churchill. He published a table with the heights of the names in feet. After converting Tyrrell's heights to the new reference, the differences were within the uncertainties of the method. To Johnston, this confirmed Tyrrell's conclusion as to the absence of any definite indications of recent land uplift. This is in contrast to results of a field survey carried out by Stanley (1939), who confirmed Bell's (1896)

evidence of unrotten driftwood ∼25 m above sea level, although he admitted the slowness of decay in the cold climate.

Tyrrell's (1894; 1896) conclusion of no clear indications of recent land uplift around Churchill was also supported by Moore (1948), who extrapolated the line of zero vertical movement in the Great Lakes region northwards on the assumption of a roughly circular shape of this line and concluded that it should pass somewhere near Churchill. Interestingly, the results indicating present-day stability of the land around Hudson Bay were later picked up by Jeffreys (1952; 1976) as an argument against the possibility of viscous flow in the earth's interior.

In his analysis of the tide-gauge data for Churchill, Gutenberg (1941) revisited the 'Sloops Cove problem' and pointed out that Tyrrell's (1894; 1896) and Johnston's (1939) reasoning had been based on the assumption that, on May 27, 1753, the ice surface was still 4.5–4.8 m above the level of the contemporary sea. However, if the ice had broken up before that date – which had happened not infrequently in more recent years –, a land uplift of more than 3 m in 180 years would be indicated. Cooke (1942) briefly reviewed Tyrrell's qualitative evidence and concluded that Gutenberg's inference of land uplift around Churchill had been premature. In his rebuttal, Gutenberg (1942) emphasized that the indications given by Tyrrell were interpreted by him merely as excluding subsidence of the land.

Indirect evidence of the ongoing diseqilibrium of the earth was provided by Innes (1948). In his study of gravity anomalies at 23 stations in northwestern Canada, he found that the free-air gravity anomaly tends to be negative over the formerly glaciated region of Canada, with a value of −54 mGal derived for Churchill. Innes suggested that this result agrees with the notion of continuing land uplift, but pointed out that that it cannot be taken as its proof.

Manning (1951) reinvestigated the driftwood strandlines in James Bay and, in particular, studied the possibility that they might have been formed by extraordinary storm tides. His conclusion was that the appearance of the highest driftwood strandlines could only be accounted for by land uplift since their formation. Manning, therefore, essentially confirmed the explanation of the driftwood strandlines first proposed by Bell (1896).

The question of present-day land uplift around Hudson Bay was once more reviewed by Bird (1954). In addition to the evidence advanced by the earlier investigators, he quoted inhabitants of Baker Lake (north of Churchill), who had noticed that the lake had retreated since the establishment of the settlement in the 1920s. Also, older Innuit agreed that, between Chesterfield Inlet and Eskimo Point (also north of Churchill), rocks had appeared since their youth. Bird furthermore referred to archaeological sites that indicated a land uplift of $\sim$24 m since the arrival of the Dorset culture and of $\sim$9 m since the arrival of the Thule culture (no absolute ages were available to Bird).

Convincing geological evidence of continuing land uplift had to await the advent of the ^{14}C dating method in the 1950s. Of particular interest are the studies by Fairbridge and Hillaire-Marcel (1977) and Hillaire-Marcel and Fairbridge (1978). Using a staircase of 185 beach ridges found along the east coast of Hudson Bay, they constructed a continuous record of emergence from $\sim$8300 a before present (sidereal) to present time. Their result was based on a newly discovered beach cycle with a period of $\sim(45 \pm 5)$ a believed to correspond to periods of storminess and high tides. Of particular interest is that the altitudinal spacing of the shorelines becomes progressively closer as they approach the modern shoreline, indicating that land uplift has been gradually

decreasing with time. In the Richmond Gulf region, a contemporary uplift of ∼11 mm/a is indicated on the basis of this evidence.

3. Tide-gauge evidence of present-day land uplift

To monitor the long-term RSL trends on regional to global scales, tide gauges continue to be a useful technique (*e.g.* Lisitzin, 1974; Emery and Aubrey, 1991; Douglas et al., 2001). For sets of globally distributed stations, the long-term trends have recently been determined and discussed by, for example, Douglas (1991; 1997), who favours time series of at least 70 a to eliminate interannual and decadal variations. At present, estimates of the globally averaged rate of RSL-height change range between 1 and 2 mm/a, with a central value of 1.5 mm/a (*e.g.* Meier and Wahr, 2002). Whereas part of this rise is probably related to the recent melting of mountain glaciers and ice caps, the major portion appears to be caused by the thermal expansion of sea water (*e.g.* Douglas and Peltier, 2002).

An interfering contribution arises from the earth's GIA following the retreat of the last Pleistocene ice sheets. This effect is particularly obvious in the once ice-covered regions of Fennoscandia and Canada, where pronounced RSL fall caused by deglacial land uplift results. In Fennoscandia, the contemporary land uplift has been monitored by more than 40 tide-gauge stations with a record length of at least 50 a (*e.g.* Plag, 1988; Ekman, 1996; Lambeck et al., 1998). In Canada, most of the long-term tide-gauge stations are located along the east coast (Vaníček and Nagy, 1979) and, thus, away from the uplift centre. Close to the uplift centre, Churchill is the location of the only tide-gauge sta-

tion with an observation record exceeding 50 a, which will be reviewed in the following.

3.1. Previous analyses

A quantitative method of deciding the question whether the land around Hudson Bay is still rising was provided when a tide-gauge was deployed at Churchill in September 1928. The first attempt to use this type of evidence was due to Gutenberg (1941). Since the early operations were interrupted during winter due to ice, records were initially available only for the summer months. To eliminate the annual period due to melting of the ice and flow of the Churchill River, Gutenberg calculated the mean rate of RSL-height change separately for each month of the observation interval 1928–1939. His results were −39 mm/a (June), −26 mm/a (July), −22 mm/a (August), −12 mm/a (September), −30 mm/a (October) and −45 mm/a (November), which gives a mean of −29 mm/a (not calculated by Gutenberg).

Gutenberg's (1941) results were rejected by Cooke (1942), who pointed out several problems associated with the Churchill tide-gauge record. In particular, he objected that the tide gauge was not located on the open coast of Hudson Bay, which causes its record to be influenced by the inflow of the Churchill River and the narrow mouth of the harbour. Cooke therefore suggested to restrict the analysis to the months of August–October, when the river flow is low and, therefore, the differences to the open sea are likely to be small. He furthermore noted that the tide-gauge readings showed no regular change. Instead, since 1928, they had stayed essentially constant until late August or early September 1934. At this time, they showed a drop of nearly 30 cm and again stayed essentially constant afterwards. Cooke emphasized

that this is not the behaviour typical of regularly rising land. However, if the land uplift did occur in a series of jerks, then, to calculate a mean rate, it would be necessary to know more about the statistics of the ground motion than could be extracted from the short Churchill record.

In his response, Gutenberg (1942) pointed out that he had used the method of linear regression of the monthly RSL heights, separately for each month, to estimate the mean rate of RSL-height change. He also noted that local effects, such as river flow and harbour conditions, were unlikely to affect trends over 12 years. Based on linear regression, Gutenberg then calculated new rates of RSL-height change for the slightly extended observation interval 1928–1940, which were (-25.0 ± 7.5) mm/a (June–November) and (-22.5 ± 7.5) mm/a (August–October).

Since the validity of the Churchill tide-gauge record and its interpretation by Gutenberg continued to be questioned (Moore, 1948; Bird, 1954), the problem was revisited by him (Gutenberg, 1954). After once more reviewing the early studies by Tyrrell (1894; 1896) and Johnston (1939), Gutenberg first noted that one reason for continuing objections to the hypothesis of contemporary land uplift around Hudson Bay appeared to be that observations on the North American continent were much more sparse and had been misinterpreted much more frequently than for Fennoscandia. Gutenberg then concluded that the studies by Tyrrell, Johnston and others suggesting stability were consistent with a moderate land uplift, but that the errors involved were too large for a reliable numerical value. In view of the inconclusive historical and geological evidence, Gutenberg advanced a new interpretation of the Churchill tide-gauge record. Limiting his analysis to the 'quiet' months July–September with reduced change, linear regression of the

monthly RSL heights for the observation interval 1929–1951 returned (-10.5 ± 1.8) mm/a as the mean rate of RSL-height change.

Later, Gutenberg (1958) discussed the Churchill tide-gauge data for the last time and considered the irregularity of the record as typical of such records and probably related to 'meteorological' influences. He also pointed out that a temporary blocking of the subcrustal flow causing the land uplift might be responsible for this irregularity. Nevertheless, the accuracy of the Churchill tide-gauge readings continued to be questioned and the rates calculated by Gutenberg continued to be regarded as unreliable (Bird, 1959; Farrand and Gajda, 1962).

A fresh attempt to analyse the Churchill tide-gauge data was undertaken by Barnett (1966). As he pointed out, the data from Churchill were probably among the least reliable, but among the most significant in support of Gutenberg's (1941) conclusion of continuing land uplift in North America. In a brief review of the technical aspects, Barnett noted that, until 1940, the tide gauge had been operated in the summer months by different agencies for the Department of Mines and Technical Surveys. During that time, instrumental set-up procedures were potential sources of error. Also, the original records did not show indications of regular level controls each time the gauge had been moved. After 1940, the operation was transferred to MSB belonging to the same department, and an automatic tide gauge was put into operation. At the same time, the records were referred to the permanent bench mark 566-D at Cape Merry, and the topographic height of the instrument was checked annually by levelling. Furthermore, a continuous record became possible by maintaining the tide gauge in a heated well connected with the sea in the winter and operating it in the harbour wharf in the summer. In 1956, the instrument was relocated and remained at the

same position all year round. In 1963, it was moved to a special gauge house.

In view of the operational problems before 1940, Barnett (1966) restricted his analysis of the Churchill tide-gauge data to the observation interval 1940–1964 and, based on linear regression of the full set of monthly RSL heights, calculated a mean rate of RSL-height change of −6.1 mm/a. A later check revealed that the rate was in fact −4.1 mm/a for this interval and −3.9 mm/a for the extended interval 1940–1968 (Barnett, 1970). This value agrees with that obtained by Dohler and Ku (1970), whose linear-regression analysis for the observation interval 1940–1967 returned (-3.9 ± 0.7) mm/a. Obviously, the new rates are significantly less than those determined by Gutenberg (1941; 1942; 1954).

Walcott (1972) discussed Barnett's (1970) estimate of the mean rate of RSL-height change at Churchill and noted that it was smaller in magnitude than the relative rates inferred from tide gauges for the Lake Superior basin. Walcott therefore concluded that the Churchill value must be treated with caution. If correct, however, it would indicate that the region of largest uplift has migrated south-east during the last several thousand years. When compiling a map of recent crustal movement for Canada, Vaníček and Nagy (1979) analysed the extended observation interval 1940–1975 using monthly RSL heights provided by MEDS. Also based on linear regression, they calculated a mean rate of RSL-height change of (-4.5 ± 0.4) mm/a for Churchill and, thus, essentially confirmed Barnett's (1970) results.

The first indication of a larger present-day land uplift resulted from the relevelling of bench mark 566-D at Cape Merry by the GSD in 1978. As Hansell et al. (1983) reported, a land-uplift rate of 8.15 mm/a was obtained from this survey.

More than a decade later, Tushingham (1992) presented another reanalysis of the Churchill tide-gauge record. Employing monthly RSL heights from MEDS and linear regression, he obtained a mean rate of RSL-height change of (-8.3 ± 0.8) mm/a for the extended observation interval 1940–1991. Since the Churchill record is expected to be influenced by annual changes, he also computed rates based on the monthly RSL heights for particular months, which ranged from ~ -7 mm/a (February) to ~ -10 mm/a (December). A possibly significant complication mentioned by Tushingham concerns the Churchill River Diversion Project between 1975 and 1977, which resulted in the flooding of vast regions ∼300 km upriver and a ∼60% diversion of the runoff of Churchill River into Nelson River further south. Since a positive correlation was found between the rate of discharge for Churchill River and the RSL height at Churchill harbour, this drastic reduction in outflow may have had a significant effect on the tide-gauge record. To study the potential effect of the diversion, Tushingham divided the complete observation interval into pre- and post-diversion intervals and obtained rates of (-4.4 ± 0.5) mm/a (1949–1975) and (-8.8 ± 2.4) mm/a (1977–1991). As he pointed out, the pre-diversion rates compare favourably with the rates determined by Barnett (1966; 1970) and Vaníček and Nagy (1979), whereas the post-diversion rates are probably unreliable because of the shortness of the record and its gaps. The various estimates of the observational mean rate of RSL-height change, $\bar{\dot{s}}_{\mathrm{obs}}$, their standard error, ϵ, and standard deviation, σ, are listed in Table I.

Table I

The most recent analysis is due to Gough and Robinson (2000). Studying the annual variation of the Churchill tide-gauge record more closely, they pointed out that it is characterized by a double amplitude of ∼300 mm before 1975 and ∼350 mm after 1975. Based on statistical

analysis, they found that the Churchill River discharge is responsible for ∼43% of this variability, whereas ∼18% are contributed by the Nelson River discharge. The increase in the annual variation after 1975 could be linked to the Churchill River diversion after 1975. In their discussion of linear trends, Gough and Robinson divided the observation interval into 1950–1970, 1970–1985 and 1985–1998 and estimated the rate of RSL-height change as −3 to −4 mm/a, −20 mm/a and close to zero, respectively, for the three sub-intervals. In contrast to Tushingham (1992), they argued that the Churchill River diversion occurred too late to be responsible for the increased RSL fall beginning in 1970. In their search for an alternative explanation, they pointed out that, during 1960–1975, the global mean temperature dropped, whereas, after 1975, it rose. Considering continental ice-mass changes and thermal expansion of the ocean water with a lag of 10 a, they showed that the expected RSL-height change is roughly consistent with the changes in linear trend observed.

3.2. New analysis based on psmsl time series

Whereas Tushingham (1992) considered MEDS data for 1940–1991, monthly RSL heights are now available from PSMSL for 1940–2001 via internet (http://www.pol.ac.uk/psmsl/). Figure 1 shows the PSMSL time series of monthly RSL heights for Churchill. An annual cycle nearly proportional to $-\sin\omega t$, where t is the time with respect to the beginning of a calendar year, with an amplitude of ∼96 mm is indicated.

Figure 1

To calculate the mean rate of RSL-height change, linear regression of the monthly RSL heights is used. Following Vaníček and Nagy (1979),

we approximate the time series by

$$s_{\mathrm{LR}}(t) = a + \bar{\dot{s}}_{\mathrm{obs}} t, \tag{1}$$

where s_{LR} is the RSL height based on linear regression, a the intercept, $\bar{\dot{s}}_{\mathrm{obs}}$ the observational mean rate of RSL-height change and t the time epoch. From linear regression, we have

$$a = \frac{\sum s_n - \bar{\dot{s}}_{\mathrm{obs}} \sum t_n}{N}, \tag{2}$$

$$\bar{\dot{s}}_{\mathrm{obs}} = \frac{N \sum t_n s_n - \sum t_n \sum s_n}{N \sum t_n^2 - (\sum t_n)^2}, \tag{3}$$

where s_n is the monthly RSL height for the nth month, t_n the reference time epoch for s_n (taken at the mid-epoch of the month) and N the total number of monthly values considered. The standard deviation, σ, of s_{obs} is given by

$$\sigma = \sqrt{\frac{\sum s_n^2 - a \sum s_n - \bar{\dot{s}}_{\mathrm{obs}} \sum t_n s_n}{N-2}}\,. \tag{4}$$

The standard error, ϵ, of $\bar{\dot{s}}$ is calculated according to

$$\epsilon = \sqrt{\frac{N\sigma^2}{N \sum t_n^2 - (\sum t_n)^2}}\,. \tag{5}$$

Linear-regression analysis for the complete observation interval ($N =$ 642 monthly RSL heights for 732 months = 61 a) yields a mean rate of RSL-height change of $\bar{\dot{s}}_{\mathrm{obs}} = (-9.72 \pm 0.26)$ mm/a with a standard deviation of $\sigma = 116$ mm (Table II). Also listed are the mean rates of RSL-height change for the sub-intervals 1940–1975 and 1975–2001. As found by Tushingham (1992), the value of $\bar{\dot{s}}_{\mathrm{obs}} = (-4.44 \pm 0.45)$ mm/a for the first sub-interval is much smaller in magnitude than that of $\bar{\dot{s}}_{\mathrm{obs}} = (-10.41 \pm 0.95)$ mm/a for the second sub-interval. Table II

To improve the result, the IB reduction (*e.g.* Lambeck, 1980) is applied to the Churchill tide-gauge data. The air-pressure data base used

for this reduction is GMSLP2.1f (Basnett and Parker, 1997), which is a global archive of historical, monthly sea-level pressure data provided by BADC. The air-pressure data are gridded with a spatial resolution of $5^\circ \times 5^\circ$, the observation interval is 1871–1994. Since the geographical coordinates of the tide-gauge station at Churchill are 58.78°N, 94.20°W, the closest grid-point in GMSLP2.1f is 60°N, 95°W.

The IB reduction is based on the assumption that the air-pressure variations change the sea level hydrostatically. Numerically, the reduction adds 1 cm to the RSL height per 1 mbar pressure in excess of 1013 mbar and vice versa. Values for the mean rate of RSL-height change for the sub-interval 1940–1994 with and without IB reduction are also given in Table II. Whereas there is only a small difference in the rates (−9.65 mm/a with IB reduction versus −9.43 mm/a without IB reduction), the standard deviation, σ, is markedly smaller if the IB reduction is applied (102 mm with IB reduction versus 115 mm without IB reduction).

3.3. Continuous-wavelet analysis

To investigate whether the Churchill tide-gauge record contains periodic signals, the PSMSL data are further analysed using the continuous-wavelet transform. This type of transform can be interpreted as a truncated Fourier transform applied to a sliding time interval (*e.g.* Hubbard, 1997; Torrence and Compo, 1998).

Figure 2 displays the residual PSMSL time series of monthly RSL heights obtained after subtracting the linear trend, the analysing Morlet wavelet, the wavelet scalogram, *i.e.* the complex modulus of the amplitude, and the Fourier amplitude spectrum. Clearly shown are the annual and sub-annual periods of 1 a, 0.5 a and 0.33 a as well

as a decadal period of ∼50 a. The latter is close to the period of ∼45 a noted by Fairbridge and Hillaire-Marcel (1977) when studying the late- and post-glacial land uplift along the east coast of Hudson Bay. In agreement with Figure 1, the amplitude of the annual oscillation increases towards the end of the observation interval considered. Also shown is the scalogram obtained after application of the IB reduction. As expected, the amplitude of the annual period is significantly reduced in this case, whereas the other features are essentially preserved. Figure 2

3.4. Linear-trend analysis

The annual RSL heights at Churchill (Figure 3) show a pronounced drop starting ∼1970 and continuing for almost 15 a. After this, the annual means have remained nearly constant. To study the variability of the calculated linear trends systematically, we use the newly developed linear-trend analysis diagram (Figure 4). It shows, in a triangle, the mean rate of RSL-height change, calculated according to the method outlined in Sec. 3.2, as a function of the length of the observation interval considered and of its mid-epoch. Grey regions inside the triangle indicate intervals for which the hypothesis of a linear trend is refused. For a fixed interval length, the diagram displays the time dependence of the linear trend, whereas, for a fixed mid-epoch, its dependence on the interval length is shown. At the bottom corner of the triangle, the linear trend for the complete observation interval is given. Figure 3 Figure 4

Obviously, short observation intervals are not suitable for estimating the long-term rate of RSL-height change, because the value depends on the mid-epoch considered. For intermediate observation intervals of ∼15 a, the diagram continues to show non-uniformity, with rates of ∼−5 mm/a for mid-epochs of 1950–1970 and rates of ∼−10 mm/a

for mid-epochs after 1985, which essentially confirms the results shown in Tables I and II. For the observation interval 1970–1985, rates in the range of −15 to −20 mm/a apply. As discussed by Gough and Robinson (2000), the interannual and decadal RSL variations visible in Figures 2 and 4 probably represent steric effects caused by temperature or salinity variations in Hudson Bay. With increasing interval length, the different rates gradually merge. Thus, for 40 a intervals, a monotonous increase in the rate of RSL fall followed by a levelling-off towards the end of the complete observation interval results.

Although the previous discussion has shown that anthropogenic activities and ocean-dynamical processes are likely to influence the tide-gauge record of Churchill, we assume that the linear trends determined for the complete time interval predominantly reflect GIA. As the most reliable rate of RSL-height change, the value of (9.65 ± 0.28) mm/a obtained after IB correction is taken.

4. Absolute-gravimetry and GPS evidence of present-day land uplift

An indirect method of monitoring GIA became available with the advent of absolute gravimetry. In Canada, an absolute-gravimetry program was initiated during the late 1980s (Lambert et al., 1989) and, recently, mean rates of gravity change have been estimated for the stations Churchill, Flin Flon, Pinawa, International Falls, Wausau and Iowa City located on a north–south traverse in mid-continental North America (Lambert et al., 2001). For most stations, the time series are only ∼5 a long with, typically, one measurement per year. An exception

is Churchill, where measurements have been taken for more than a decade and also more frequently.

Compared to Fennoscandia, where a rather dense network of GPS stations in operation for ∼10 a has returned accurate rates of change of the displacement field (Scherneck et al., 2002), the situation is less favourable in Canada. Over the last several years, IGS stations have been in operation at Algonquin Park, Churchill, Flin Flon, Ottawa, Schefferville, St. John's, Whitehorse and Yellowknife. After 2000, they were supplemented by new stations at Baie Comeau, Baker Lake, Halifax, Kuujuarapik, Pickle Lake and Val d'Or jointly operated by GFZ and GSD.

In the following, only Churchill will be considered, where absolute-gravimetry and GPS observations started in 1987 and 1993, respectively.

4.1. Previous analyses

To provide independent evidence of present-day isostatic adjustment, Lambert et al. (1994) proposed an analysis of temporal gravity variations based on absolute gravimetry at Churchill conducted during nine campaigns between 1987 and 1991. Upon elimination of one anomalous value, linear regression returned a rate of gravity change of -1.6 μGal/a with a standard deviation of 2.0 μGal. Later, as more absolute-gravimetry data had become available, Lambert et al. (1996) presented a new value. Disregarding two anomalous measurements in 1990, they estimated a rate of gravity change of (-1.45 ± 0.19) μGal/a and a standard deviation of 1.6 μGal for the observation interval 1987–1995. Lambert et al. (1998) tried to improve the constraints on GIA in Manitoba by combining three types of observation: the late-glacial tilting

of the Campbell shoreline of pro-glacial Lake Agassiz, the present-day tilting of southern Manitoba lakes and the present-day rate of gravity change at Churchill for the observation interval 1987–1995. Eliminating another gravity measurement regarded as anomalous and using weighted linear regression (which allows for a constant bias for each gravimeter used), they obtained an improved rate of gravity change of (-1.63 ± 0.17) μGal/a. Using the conversion factor -6.7 mm/μGal obtained from theoretical predictions, this corresponds to a rate of topographic-height change of (10.9 ± 1.1) mm/a. Lambert et al. (1998) also compared this value with Tushingham's (1992) linear-trend estimates of the mean rate of RSL-height change for Churchill, where one of his values was $\sim(-8.5 \pm 1.0)$ mm/a. If corrected for an estimated rate of globally averaged RSL-height change of 1.5 mm/a and a calculated rate of local geoid-height change of 0.9 mm/a, this returned a rate of topographic-height change of (10.9 ± 1.0) mm/a. Recently, Lambert et al. (2001) have analysed 71 gravity measurements made at six sites along a profile from Hudson Bay to Iowa during the observation interval 1987–1999. Weighted linear regression gave a rate of gravity change of (-2.13 ± 0.23) μGal/a for Churchill. This is significantly higher than predicted using ice model ICE-3G and a 'standard' earth model (Tushingham and Peltier, 1991). Lambert et al. (2001) noted that the discrepancy can be avoided either by an increase of the lower-mantle viscosity by a factor of $\sim$2 or by a 50% increase in thickness of ICE-3G on the Canadian Shield west of Lake Superior.

Larson and van Dam (2000) analysed data from four locations in Canada and the northern USA based on at least three years of continuous GPS observations and at least two absolute-gravimetry campaigns. Although gravity changes may reflect mass changes not recorded by GPS, the mean rates determined by the two techniques agree within the

standard errors at all sites (using the conversion factor -6.5 mm/μGal). The mean rates of topographic-height and gravity change determined for Churchill are, respectively, (10.7±0.23) mm/a and (-1.54±0.48) μGal/a (estimated from their Figure 4). Park et al. (2002) analysed GPS data for 20 selected IGS stations in north-eastern USA and mid-western Canada and determined mean rates of topographic-height change by linear regression. For the least-squares fit of the estimated rates by predictions based on glacial-isostatic adjustment, the estimate of (13.0 ± 0.33) mm/a for Churchill was too high by ∼3 mm/a.

The various estimates of the observational mean rates of topographic-height change, $\bar{\dot{u}}_{\rm obs}$, and gravity change, $\bar{\dot{g}}_{\rm obs}$, their standard error, ϵ, and standard deviation, σ, are listed in Table III. Table III

4.2. New GPS analysis based on IGS solutions

The GPS station Churchill (CHUR, 58.75°N, 94.08°W) has been operated by GSD with a continuous observation history since April 24, 1993. CHUR is one of the 273 globally distributed GPS stations selected by GFZ for various research projects. The data are processed on a daily basis using the program `epos` (Gendt et al., 1994) developed by GFZ. For the present study, the output of `epos` are loosely constrained daily network solutions. Back to 1996, the data have been analysed in three routines. The first routine processes the data with a one-week delay. The second routine processes the data with a 460-day delay to include late data. The third routine processes the data backwards every four weeks to obtain a quick overview of the time series. The contributions from the three routines to the time series are: 50102–

52028 MJD, 52028–52510 MJD and 52510–52964 MJD[1] for routines 3, 2 and 1, respectively. To reduce the computing time for data processing, the 273 GPS stations are grouped into four clusters. Each cluster itself constitutes a global network consisting of 80–100 stations. There are ∼30 stations that are common to all clusters and used for combining the cluster solutions to the whole-network solution.

To determine the site velocities, position time series are constructed for each site separately from daily or weekly solutions, from which the site velocities are obtained by linear regression (Zhang, 1996; Dong et al., 2002). The advantage of this method is that it allows the identification of position outliers. Moreover, any misfit for one site does not affect the estimates for the other sites.

To transform the time series into a unified reference frame, we refer the loosely constrained daily solutions to ITRF2000 (Altamimi et al., 2002) by a seven-parameter Helmert transformation:

$$\begin{bmatrix} X \\ Y \\ Z \end{bmatrix}_{\mathrm{ITRF}} = (1+c)\left(\begin{bmatrix} t_X \\ t_Y \\ t_Z \end{bmatrix} + \begin{bmatrix} 1 & r_Z & -r_Y \\ -r_Z & 1 & r_X \\ r_Y & -r_X & 1 \end{bmatrix} \begin{bmatrix} X \\ Y \\ Z \end{bmatrix}_{\mathrm{LCRF}}\right), \tag{6}$$

where (X, Y, Z) are the daily position coordinates, (t_X, t_Y, t_Z) the translation components, (r_X, r_Y, r_Z) the rotation angles, c is a dimensionless scaling term and the subscripts ITRF and LCRF indicate Cartesian coordinates in ITRF2000 and the loosely constrained reference frame, respectively. In total, 65 globally distributed high-quality core stations (Figure 5) are used for estimating the seven parameters of the Helmert transformation. Before it is implemented, the station coordinates given

Figure 5

[1] The Julian Date (JD) is defined as the number of days elapsed since January 1, 4713 BC, 12:00 h UT. The Modified Julian Date (MJD) is defined as JD − 2400000.5 d.

in ITRF2000 must be mapped to the epoch of the daily solution.

Subtracting mean position coordinates, $(\overline{X}, \overline{Y}, \overline{Z})$, from the daily position coordinates, $(X, Y, Z)_{\mathrm{ITRF}}$, gives the time series of residual position coordinates, $(\Delta X, \Delta Y, \Delta Z)$, in a body-fixed reference system. From this, time series for east, north and topographic-height coordinates, $(\Delta E, \Delta N, \Delta H)$, are obtained by transforming the residual coordinates from the body-fixed to a topocentric coordinate system:

$$\begin{bmatrix} \Delta E \\ \Delta N \\ \Delta H \end{bmatrix} = \begin{bmatrix} -\sin\lambda & \cos\lambda & 0 \\ -\cos\lambda\sin\varphi & -\sin\lambda\sin\varphi & \cos\varphi \\ \cos\lambda\cos\varphi & \sin\lambda\cos\varphi & \sin\varphi \end{bmatrix} \begin{bmatrix} \Delta X \\ \Delta Y \\ \Delta Z \end{bmatrix}, \qquad (7)$$

where λ and φ are the station longitude and station latitude, respectively.

Before estimating the linear trend for CHUR, its topographic-height time series is further analysed. This, in particular, requires the consideration of topographic-height changes caused by ocean loading, where the ocean-tide model FES95.2 is used. Also, semi-annual and annual sinusoidal waves must be removed, which have been found to contribute significantly to the variations of the station coordinates (*e.g.* van Dam et al., 2001; Crétaux and Soudarin, 2002; Dong et al., 2002; Zhang and Dong, 2002) and, thus, to influence the estimation of the linear trends (Blewitt and Lavallée, 2002). The offset observed for CHUR at 51902 MJD (December 24, 2000) is taken into account by a Heaviside step function with a jump of (-5.3 ± 0.22) mm (Figure 6). Finally, a weighted least-squares method is used for determining the observational mean rate of topographic-height change, $\bar{\dot{u}}_{\mathrm{obs}}$ and its standard error, ϵ, with the values of the time-series weighted according to their formal errors. Apart from the weighting, the procedure follows that outlined for the RSL height. The new rate is (11.4 ± 0.7) mm/a, which is close to the value of 10.7 mm/a obtained by Larson and van Dam (2000),

Figure 6

but does not confirm that of 13.0 mm/a given by Park et al. (2002) (Table III). However, the last value is probably less reliable, because no allowance was made for sinusoidal contributions.

The accuracy of the mean rate of topographic-height change estimated for CHUR may be improved by taking variations due to atmospheric loading into account. The problem goes back to Rabbel and Zschau (1985), who suggested atmospheric-pressure reductions to measurements of topographic height and gravity. van Dam and Wahr (1987) and van Dam et al. (1994) further studied the problem and found that peak-to-peak topographic-height changes caused by atmospheric-pressure variations may reach 15–20 mm. Besides semi-annual and annual variations automatically taken into account by fitting sinusoidal waves, the main contributors are storm-induced topographic-height changes dominated by periods of about two weeks. The application of appropriate corrections reduced the standard deviation of the estimates for ∼60% of the investigated GPS stations (van Dam et al., 1994; Brondeel and Willems, 2003). However, the results achieved are not completely satisfactory yet, the main reasons probably being inadequate atmospheric-pressure data or unrealistic earth models. For this reason, no atmospheric-loading reduction has been applied to the GPS data for CHUR so far.

5. SLI evidence of late- and post-glacial RSL height

In Canada, many marine features and associated organic materials had long been recognised as indicators of RSL-height changes. Since the first application of ^{14}C dating to the organic materials during the 1950s, it has become generally accepted that their age is late- or post-glacial.

However, most samples provide only bounds for estimates of past sea levels. Thus, a marine shell indicates that the contemporaneous sea level lay above its topographic height, whereas a terrestrially deposited peat indicates that the sea level lay below its topographic height. In the following, any indicator of late- or post-glacial RSL height will be referred to as SLI.

5.1. Hudson Bay region

Early compilations of dated SLIs for Canada, including the north-eastern USA, were provided by Farrand (1962), Walcott (1972) and others. On the supposition that the RSL height varies gradually with location, the SLIs were grouped into regions (Figure 7) and RSL diagrams constructed for each region (see Figure 8 for Churchill).

Figure 7

Attempts to estimate relaxation times for the Hudson Bay region on the assumption of an exponential RSL-height change go back at least to Walcott (1980), who constructed an RSL diagram for region HM[2] in southern Hudson Bay and calculated a relaxation time of >5.0 ka. This differs from the results of Mitrovica and Peltier (1993), who estimated much shorter relaxation times of 2.5, 3.3 and 2.0 ka for regions OI, SI and UP, respectively, in northern Hudson Bay. Mitrovica and Peltier (1995) considered a larger assembly of regions in Hudson Bay. Whereas they retained the relaxation times for regions OI and UP, their new estimates for regions HM and SI were 17.9 and 4.9 ka, respectively. In addition, they determined relaxation times for the following regions: CH: 5.6 ka, JB: 1.5 ka, KW: 28.6 ka and RG: 7.6 ka (see also Peltier, 1994). In their inversion, Mitrovica and Peltier ignored the relaxation times for regions CH and KW, because the SLIs they regarded as

[2] For abbreviations of the region names see Figure 7 and Appendix B.

reliable span only time intervals of 3.0 and 1.2 ka, respectively. For the remaining regions, the agreement was found to be better in the north than in the south.

For a new inversion, Peltier (1996) disregarded the long relaxation time for region HM and drastically reduced the relaxation time for region KW to (5.73±4.60) ka (presumably based on a different selection of SLIs). His revised estimates for the remaining regions are as follows: CH: (5.70 ± 2.02) ka, JB: (3.64 ± 0.68) ka, OI: (3.06 ± 0.52) ka, RG: (7.23 ± 3.18) ka, SI: (4.69 ± 1.61) ka and UP: (3.34 ± 0.83) ka.

In view of the heterogeneity of the relaxation-time estimates, Peltier (1998) constructed a composite RSL diagram for region SE along the south-east coast of Hudson Bay. It is based on SLIs collected over the broad region covering 51.5°–56.5°N and 76.5°–79.0°W and encompasses regions JB and RG. The relaxation time he obtained is 3.43 ka. He slightly reduced the relaxation time for region JB, the new value being 3.40 ka. Later, Peltier (1999) proposed three revised estimates: (3.26 ± 0.12) ka for region JB, (4.68±0.19) ka for region RG and (3.90±0.07) ka for region SE.

Reviewing the estimates, Mitrovica et al. (2000) argued that Peltier's (1998; 1999) results for region SE are questionable, because they are based on SLIs distributed over a large area stretching ∼600 km. At the same time, they pointed out a number of errors in previous estimates of relaxation times. Using revised compilations of SLIs and taking into account eustatic sea-level changes, they inferred values of (2.4 ± 0.4) ka and (5.3 ± 1.3) ka for regions JB and RG, respectively.

Fang and Hager (2002) also noted that the relaxation-time estimates proposed by Peltier (1998; 1999) for region SE are markedly smaller than previous estimates for region RG (Peltier, 1994; Mitrovica and Peltier, 1995; Peltier, 1996). Similar to Mitrovica et al. (2000), they

listed several doubtful assumptions as responsible for the reduced values. In particular, they questioned Peltier's storm-beach correction in the form of uniformly lowering all RSL heights by ∼6 m irrespective of the type of SLI the heights are based on. For their own estimate, Fang and Hager used the RSL data without correction, but limited the time window to 6.8 ka, resulting in a relaxation time of (6.3 ± 1.0) ka for region RG.

The estimates of the relaxation time for the Hudson Bay region are listed in Table IV. Table IV

5.2. Churchill region

The present study uses the SLI data base compiled for Canada by A. Dyke (pers. comm.) and is limited to 25 SLIs for region CH (Table V). In the following, an SLI will represent a sample indicative of Table V post-glacial sea level, for which latitude, φ, longitude, λ, RSL height (with respect to present-day sea level), $s_{\rm obs}$, ^{14}C age, $t_{\rm C14}$, and its standard error, $\epsilon_{\rm C14}$, have been determined. Depending on the type of sample, in our case shell (20), peat (2), bone (1), charcoal (1) or wood (1), and the type of deposition environment, an individual sample may represent an upper bound, a lower bound or a finite range for the RSL height at the time of deposition. The ^{14}C ages are reservoir corrected and based on a half-life of 5570 a. The calibrated ages correspond to the 'true' time of deposition before 1950. They are determined from $t_{\rm C14}$ and $\epsilon_{\rm C14}$ using the 2σ-calibration mode of the program program `calib 4.1` (Stuiver and Reimer, 1993) providing upper and lower bounds, $t_{\rm cal}^{\rm max}$ and $t_{\rm cal}^{\rm min}$, respectively. The calibrated ages themselves and their standard errors then follow from $t_{\rm cal} = (t_{\rm cal}^{\rm min} + t_{\rm cal}^{\rm max})/2$ and $\epsilon_{\rm cal} = (t_{\rm cal}^{\rm max} - t_{\rm cal}^{\rm min})/2$, respectively.

Conventionally SLIs from a particular region are combined in an RSL diagram displaying the time dependence of their RSL heights (Figure 8). In contrast to previous studies (*e.g.* Tushingham, 1992), where the RSL diagram refers to some average position, we retain the actual positions of the SLIs considered, because they are distributed over a region of $\sim(200 \times 200)$ km^2 (Figure 9).

Figure 8

Figure 9

6. Estimates of mantle viscosity

Whereas qualitative models of the process of GIA date back to the 19th century (see Wolf, 1993, for a historical review), quantitative models allowing estimates of the mantle viscosity have largely been developed after 1970 (see Peltier, 1998, 2004; Sabadini and Vermeersen, 2004, for a historical review). At the beginning, most viscosity estimates were fully based on the late- and post-glacial RSL history documented by an increasingly dense global distribution of SLIs. More recently, the present-day adjustment recorded by ground-based or satellite-based geodetic techniques has been included as an additional constraint on the viscosity distribution.

In the following compilation, only those previous estimates of mantle viscosity that are either exclusively or predominantly based on the SLI evidence from the Hudson Bay region will be considered.

6.1. Previous estimates

Irrespective of the inconsistencies associated with the SLIs from the Hudson Bay region (Figure 7), attempts to infer the mantle viscosity from the data are numerous. One of the first interpretations is due to

Nakada (1983), who considered regions CH, HM, OI and SI. Fixing the upper-mantle thickness below the lithosphere to 200 km and the lower-mantle viscosity to 10^{23} Pa s, he found that the upper-mantle viscosity required for the Hudson Bay region ranges between 0.05 and 0.75×10^{21} Pa s. If region CH is considered separately, the upper-mantle viscosity inferred is $\sim 0.5 \times 10^{21}$ Pa s. As Nakada pointed out, these models also satisfy the free-air gravity anomaly observed over Hudson Bay, which is, however, more recently believed to be partially related to mantle convection (Mitrovica, 1997; Simons and Hager, 1997).

Peltier and Andrews (1983) considered RSL data from regions CH, RG and OI supplemented by data from region EC and and the free-air gravity anomaly over Hudson Bay. They found that upper- and lower-mantle viscosities of 10^{21} Pa s and $(1\text{–}3) \times 10^{21}$ Pa s, respectively, fit the data most closely. The reduced viscosity values in the lower mantle were found to be compatible also with the free-air gravity anomaly. Peltier and Andrews explained this by the excitation of internal relaxation modes associated with the density stratification of the earth model used.

Nakada and Lambeck (1991) examined whether the upper-mantle viscosity varies globally and presented preliminary results for four regions in terms of an earth model with a two-layer mantle separated by a discontinuity at 670-km depth. Considering RSL data from regions CH, HM and OI, they found that optimum fits are obtained for $\eta_{\mathrm{UM}} = (0.4\text{–}0.6) \times 10^{21}$ Pa s and $\eta_{\mathrm{LM}} = (20\text{–}50) \times 10^{21}$ Pa s.

Mitrovica and Peltier (1992) studied the depth resolution of the RSL data from the Hudson Bay region. Disregarding the free-air gravity anomaly, they showed that the RSL history for regions JB, KW, OI, RG, SI and UP can be explained by a model with an upper-mantle viscosity of 10^{21} Pa s and a lower-mantle viscosity of $(1\text{–}3) \times 10^{21}$ Pa s,

thus confirming the result of Peltier and Andrews (1983). Investigating the sensitivity kernels, they also showed that the data are most sensitive to viscosity variations in the very deepest regions of the upper mantle and in the top half of the lower mantle. With a two-layer lower mantle, the lower-mantle viscosity above 1800-km depth was found to be $\sim 10^{21}$ Pa s, but a significant increase at larger depths cannot be ruled out.

Mitrovica and Peltier (1993) continued their study of the resolving power of the Hudson Bay RSL data on the basis of their estimates of the relaxation times for regions OI, SI and UP. Using a time window extending 6 ka backwards from today, their inversion confirmed the limited resolution in the bottom half of the lower mantle. The mean viscosity inferred for the depth interval between 500 and 1870 km is $(0.66\text{–}1.2) \times 10^{21}$ Pa s.

Han and Wahr (1995) returned to the conventional viscosity parameterization in terms of two uniform layers separated by the 670-km discontinuity and considered RSL data from regions CH, HM, KW, OI, SI and UP supplemented by the free-air gravity anomaly over Hudson Bay. Using a single-disk model of the Laurentide ice sheet, they concluded that it is not possible to fit the RSL data from the six sites simultaneously. Best results were obtained for an upper-mantle viscosity of 0.6×10^{21} Pa s and a lower-mantle viscosity of 30×10^{21} Pa s. With an ice-sheet model consisting of four subdomes, a slightly improved fit of the data was achieved for an upper-mantle viscosity of 1.0×10^{21} Pa s and a lower-mantle viscosity of 50×10^{21} Pa s. If the free-air gravity anomaly was ignored, Han and Wahr could not rule out the value of 10^{21} Pa s for the lower-mantle viscosity.

Mitrovica and Peltier (1995) interpreted RSL data from regions HM, JB, OI, RG, SI and UP. Based on forward calculations, they found that,

for two mantle layers separated by the 670-km discontinuity, the lower-mantle viscosity is in the range of $(0.5–3)\times10^{21}$ Pa s. The upper-mantle viscosity was poorly resolved, but probably $\sim0.5\times10^{21}$ Pa s. However, similar to other investigators, Mitrovica and Peltier concluded that no single earth model can reconcile the RSL record from all regions. Since the record for region HM appeared to be problematic due to a large time gap, it was excluded from the inverse modelling. The solution to the inverse problem for the depth interval of maximum sensitivity to viscosity variations between 500 and 1800 km resulted in viscosities between 0.71 and 1.1×10^{21} Pa s.

Forte and Mitrovica (1996) carried out joint inversions based on RSL data from region RG near the previous glaciation centre in Canada, RSL data from Fennoscandia and convection-related global data. The viscosity profiles constructed show a significant jump by a factor of $\sim$10 near 1000-km depth. Between the surface and 1400-km depth, the viscosity was found to be 0.76×10^{21} Pa s. For the depth interval 400–1800 km, a value of 1.9×10^{21} Pa s was obtained.

Focussing on RSL data from region RG and based on forward calculations, Mitrovica (1996) showed that the RG relaxation time requires a lower-mantle viscosity of $>2.4\times10^{21}$ Pa s. Based on a joint inversion of the RSL data from region RG and Fennoscandia, he furthermore demonstrated that the weighted mean of the viscosity between 670-km and 2000-km depth is $(1.4–3.3)\times10^{21}$ Pa s, whereas the viscosity increase between the upper mantle and the top 1000 km of the lower mantle is more than one order of magnitude. A joint inversion of relaxation times for regions OI, SI, UP and Fennoscandia resulted in a weighted mean of the viscosity between 670-km and 2000-km depth of $\sim0.79\times10^{21}$ Pa s.

Cianetti et al. (2002) interpreted the RSL data from regions CH, HM, JB, KW, OI, RG, SI and UP. Based on forward modelling, they found that the data can be reconciled by an upper-mantle viscosity of 10^{21} Pa s and a lower-mantle viscosity of 2×10^{21} Pa s. Using an inverse approach based on the Metropolis sampling algorithm, they further showed the RSL data from region CH suggest an essentially uniform mantle with upper- and lower-mantle viscosities of 3.2×10^{21} Pa s and 4.0×10^{21} Pa s, respectively. As in previous studies, it was not possible to infer viscosity profiles that simultaneously matched RSL data from all regions within their uncertainties. The closest fit was reached for upper- and lower-mantle viscosities of 0.16×10^{21} Pa s and 2.0×10^{21} Pa s.

Mitrovica and Forte (2002) determined viscosity profiles using Occam-type inversions of RSL data from regions JB and RG supplemented by RSL data from Fennoscandia and observables related to mantle convection. Parameterizing the mantle into 13 layers, the models obtained show a 2–3 order-of-magnitude increase in viscosity from the base of the lithosphere to 2000-km depth and a region of lower viscosity from 2000-km depth to the CMB. The mean viscosity values found were $(0.39–0.43) \times 10^{21}$ Pa s for the upper mantle and $(6.5–11) \times 10^{21}$ Pa s for the lower mantle. All inversions produced viscosity models that fit the relaxation time for RG better than the shorter relaxation time estimated for region JB, which was taken as indicative of the inferior accuracy of the latter. In a follow-up study, (Mitrovica and Forte, 2004) increased the resolution in the mantle to 25 layers and obtained similar viscosity profiles by inversion. If convection-related observables were excluded, the mean viscosities obtained were 0.5×10^{21} Pa s for the upper mantle and 1.0×10^{21} Pa s for the lower mantle.

The results of the previous interpretations of the late- and post-glacial RSL record around Hudson Bay are compiled in Table VI. Table VI

6.2. New estimate based on joint inversion

In the following determination of mantle viscosity, we will use as observables for region CH the mean rate of RSL-height change, $\bar{\dot{s}}_{\rm obs} = (-9.65 \pm 0.28)$ mm/a (present study), the mean rate of topographic-height change, $\bar{\dot{u}}_{\rm obs} = (11.35 \pm 0.7)$ mm/a (present study), the mean rate of gravity change, $\bar{\dot{g}}_{\rm obs} = (-2.13 \pm 0.23)$ μGal/a (Lambert et al., 2001), and the late- and post-glacial RSL height (Dyke, pers. comm.).

The last Pleistocene glaciation is simulated using a modified version of ice model ICE-3G (Tushingham and Peltier, 1991). The main alterations are the adjustment of the time scale and the consideration of a linear glaciation phase with a duration of 40 ka. The earth model employed is radially symmetric, self gravitating and viscoelastic, with the stratifications of the density and the elastic parameters according to PREM. To solve for the glaciation-induced perturbations of the field quantities, the spectral finite-element method (Martinec, 2000) is employed, where the earth-ice-ocean system is coupled by the sea-level equation (Wolf et al., 2002; Hagedoorn, 2005) accounting for the redistribution of melt water, geoid-height changes, moving coast lines and grounded ice. During the inversion procedure, the lithosphere thickness, $h_{\rm L}$, is kept fixed at 100 km. The upper-mantle viscosity, $\eta_{\rm UM}$, is varied between 0.1 and 3×10^{21} Pa s and the lower-mantle viscosity, $\eta_{\rm LM}$, between 0.1 and 3×10^{22} Pa s. Using these values, the rates of RSL-height change, topographic-height change and gravity change are calculated for the location of Churchill and the present time epoch, and the RSL height for the locations of the individual SLIs and the corresponding post-glacial time epochs. The program `genesis` (Hagedoorn, 2005) used provides the radial, longitudinal and latitudinal displacement components, $(u_r, u_\lambda, u_\varphi)$, respectively, the lo-

cal incremental gravitational potential, $\phi^{(\Delta)}$, and the local incremental gravity, $g^{(\Delta)}$. From these, the computational field quantities are defined:

$$\bar{\dot{u}}_{\rm com} := \frac{u_r(t_2) - u_r(t_1)}{t_2 - t_1}, \tag{8}$$

$$\bar{\dot{s}}_{\rm com} := -\frac{\phi^{(\Delta)}(t_2) - \phi^{(\Delta)}(t_1)}{g^{(0)}(t_2 - t_1)} - \bar{\dot{u}}_{\rm com}, \tag{9}$$

$$\bar{\dot{g}}_{\rm com} := -\frac{g^{(\Delta)}(t_2) - g^{(\Delta)}(t_1)}{t_2 - t_1} - \partial_r g^{(0)} \bar{\dot{u}}_{\rm com}, \tag{10}$$

where $g^{(0)} = 9.81$ m/s^2 and $\partial_r g^{(0)} = -3.086 \times 10^{-6}$ s^{-2} are the unperturbed gravity and its gradient, respectively, and all quantities are evaluated at the earth's surface. The quality of the fit is evaluated using the magnitude of the difference between the computational and observational rates:

$$\chi(\bar{\dot{f}}) := |\bar{\dot{f}}_{\rm obs} - \bar{\dot{f}}_{\rm com}|, \tag{11}$$

where $\chi(\bar{\dot{f}})$ is the misfit function for $\bar{\dot{f}}$ representing $\bar{\dot{u}}$, $\bar{\dot{s}}$ or $\bar{\dot{g}}$.

For the interpretation of the late- and post-glacial topographic-height change, the computational RSL height, $s_{\rm com}$, is compared with the corresponding observational RSL height, $s_{\rm obs}$, with the weighting of the fit controlled by the constraints given by the SLIs according to a fuzzy-logic scheme (*e.g.* Demicco and Klir, 2004). More precisely, we assume that, for each SLI, the fit is quantified by a trapezoidal membership function, w, (Figure 10). For SLIs indicating an upper bound, $w = 1$ if the computational RSL height is below the bound, $s_{\rm com} \leq s^{\rm max}_{\rm obs}$. Conversely, for SLIs indicating a lower bound, $w = 1$ if the computational RSL height is above the bound, $s_{\rm com} \geq s^{\rm min}_{\rm obs}$. For SLIs indicating a finite range, $w = 1$ if the computational RSL height is within the finite range, $s^{\rm min}_{\rm obs} \leq s_{\rm com} \leq s^{\rm max}_{\rm obs}$. The width of the linear ramps, Δs, where $0 < w < 1$, is determined according to $\Delta s = \dot{s}_{\rm com}\, \epsilon_{\rm cal}$, where $\dot{s}_{\rm com}$ is the computational rate of RSL-height change at the location and time epoch of deposition of the SLI. The

Figure 10

misfit function for the RSL height, s, is then given by

$$\chi(s) := 1 - \frac{1}{P} \sum_{p=1}^{P} w_p(s_{\rm obs}, s_{\rm com}), \tag{12}$$

where P is the total number of SLIs considered and w_p is the membership function for the pth SLI.

Figure 11 shows the computational rates of RSL-height change, topographic-height change and gravity change as well as the differences to the corresponding observational rates as functions of upper- and lower-mantle viscosities. The contour patterns for the three computational rates are similar and the best-fit regions (defined as less than one-standard deviation from the observational rates) are nearly the same. The optimum viscosity values are $\eta_{\rm UM} \sim 3.2 \times 10^{20}$ Pa s and $\eta_{\rm LM} \sim 1.6 \times 10^{22}$ Pa s. Figure 12 shows the fit achieved for the late- and post-glacial RSL height. The general pattern and best-fit region closely resemble those shown in Figure 11 and, thus, confirm the results obtained using the present-day rates.

Figure 11

Figure 12

To compare the results for the individual observables more directly, we superimpose the best-fit parameter regions successively (Figure 13). As indicated above, the rates of RSL-height and gravity change constrain the upper- and lower-mantle viscosities most closely. The best-fit regions for the rate of topographic-height change and for the late- and post-glacial RSL height are somewhat broader, but not in conflict with the results obtained for the other observables.

Figure 13

As discussed by Peltier (2004), the ice thickness in ice model ICE-3G west of Hudson Bay is probably too small. This is corrected in his revised ice model ICE-5G, which accounts for the suggested additional ice by a Keewatin ice dome. We have simulated this dome by superimposing on ICE-3G a gradually growing and decaying circular disc located at 61.5°N, 107.0°W. At the glacial maximum, it has a radius of

500 km and a central thickness of 2700 m, which corresponds to ∼5% additional ice over North America. For the optimum viscosity profile, this modification leaves the predictions of the late- and post-glacial RSL heights nearly unchanged, whereas the predicted rates of RSL-height change, topographic-height change and gravity change are enhanced by $\simeq 5\%$. This increase can be compensated by a slight reduction of the lower-mantle viscosity by a factor of < 2 – a result in agreement with that obtained by Lambert et al. (2001).

7. Summary

The main results of our study are as follows:

We have extended the analysis of tide-gauge data for Churchill carried out by Tushingham (1992) by including data from the last decade. As a new analysis tool, we have developed the linear-trend analysis diagram, which allows a systematic investigation of the linear trend in the RSL-height change as a function of the length of the observation interval and its mid-epoch. For short and intermediate observation intervals, the diagram displays considerable variability of the estimated linear trends, whence the IB-corrected mean rate of RSL-height change of (-9.72 ± 0.26) mm/a for the observation interval 1940–2001 is regarded as most reliable.

We have processed GPS data for Churchill using a time series from 1996–2001. Taking into account biannual and annual signals as well as allowing for a jump in the record, we have arrived at a mean rate of topographic-height change of (11.4 ± 0.7) mm/a.

We have considered 25 SLIs from the region CH, which are indicators of the RSL height during the past 9000 a. After analysing whether a

sample provides an upper bound, a lower bound or a finite range for post-glacial RSL height, we have designed a fuzzy scheme to improve the results.

Finally, using ice model ICE-3G, a viscoelastic earth model with the upper- and lower-mantle viscosities as free parameters and the sea-level equation, we have inverted the present-day rates of RSL-height change, topographic-height change and gravity change as well as the late- and post-glacial RSL height in terms of mantle viscosity. All four types of observable return consistent best-fit parameter regions. The optimum values are $\sim 3.2 \times 10^{20}$ Pa s and $\sim 1.6 \times 10^{22}$ Pa s for the upper- and lower-mantle viscosities, respectively. Considering the uncertainties of the individual data sets, the constraint imposed on the lower-mantle viscosity can be relaxed such that values $> 5 \times 10^{21}$ Pa s are indicated for it.

Acknowledgements

Monthly tide-gauge data from PSMSL were obtained via internet. J. Arnott and D. Parker from Hadley Centre, Meteorological Office, Bracknell, England, released the global mean sea-level pressure data. SLIs for North America were provided by A. Dyke from GSC. The method of processing GPS data at GFZ was developed by M. Ge, who partly processed the Churchill data, and by G. Gendt. The data processing was technically supported by the IGS group at GFZ responsible for software development and data preparation. F. Barthelmes at GFZ wrote the program for the continuous wavelet transform. The Graphics program GMT (Wessel and Smith, 1991) was employed. This study was

part of the SEAL project, BMBF Project No. SF2000/13. We would like to thank Erik Ivins and Patrick Wu for their thoughtful reviews.

References

Altamimi, Z., P. Sillard, and C. Boucher: 2002, 'ITRF2000: A New Release of the International Terrestrial Reference Frame for Earth Science Applications'. *Journal of Geophysical Research, Solid Earth* **107**, 2214, doi:10.1029/2001JB000561.

Barnett, D. M.: 1966, 'A Re-Examination and Re-Interpretation of Tide-Gauge Data for Churchill, Manitoba'. *Canadian Journal of Earth Science* **3**, 77–88.

Barnett, D. M.: 1970, 'An Amendment and Extension of Tide-Gauge Data Analysis for Churchill, Manitoba'. *Canadian Journal of Earth Science* **7**, 626–627.

Basnett, T. A. and D. E. Parker: 1997, *Development of the Global Mean Sea Level Pressure Data Set GSMLP2*, Climate Research, Technical Note No. 79. Exeter: Hadley Centre for Climate Prediction.

Bell, R.: 1896, 'Proofs of the Rising of the Land around Hudson Bay'. *American Journal of Science, Series 4* **1**, 219–228.

Bird, J. B.: 1954, 'Postglacial Marine Submergence in Central Arctic Canada'. *Geological Society of America Bulletin* **65**, 457–464.

Bird, J. B.: 1959, 'Recent Contributions to the Physiography of Northern Canada'. *Zeitschrift für Geomorphologie* **3**, 151–174.

Blewitt, G. and D. Lavallée: 2002, 'Effect of Annual Signals on Geodetic Velocity'. *Journal of Geophysical Research, Solid Earth* **107**, 2145, doi:10.1029/2001JB000570.

Brondeel, M. and T. Willems: 2003, 'Atmospheric Pressure Loading in GPS Height Estimates'. *Advances in Space Research* **31**, 1959–1964.

Cianetti, S., C. Giunchi, and G. Spada: 2002, 'Mantle Viscosity Beneath the Hudson Bay: An Inversion Based on the Metropolis Algorithm'. *Journal of Geophysical Research, Solid Earth* **107**, 2352, doi:10.1029/2001JB000585.

Cooke, H. C.: 1942, 'Is the Land around Hudson Bay at Present Rising?'. *American Journal of Science* **240**, 144–146.

Crétaux, J.-F. and L. Soudarin: 2002, 'Seasonal and Interannual Geocenter Motion from SLR and DORIS Measurements: Comparison with Surface Loading Data'. *Journal of Geophysical Research, Solid Earth* **107**, 2374, doi:10.1029/2002JB001820.

Demicco, R. V. and G. J. Klir (eds.): 2004, *Fuzzy Logic in Geology*. San Diego: Elsevier Academic Press.

Dohler, G. C. and L. F. Ku: 1970, 'Presentation and Assessment of Tides and Water Level Records for Geophysical Investigations'. *Canadian Journal of Earth Science* **7**, 607–625.

Dong, D., P. Fang, Y. Bock, M. K. Cheng, and S. Miyazaki: 2002, 'Anatomy of Apparent Seasonal Variations from GPS-Derived Site Position Time Series'. *Journal of Geophysical Research, Solid Earth* **107**, 2075, doi:10.1029/2001JB000573.

Douglas, B. C.: 1991, 'Global Sea Level Rise'. *Journal of Geophysical Research, Solid Earth* **96**, 6981–6992.

Douglas, B. C.: 1997, 'Global Sea Rise: A Redetermination'. *Surveys in Geophysics* **18**, 279–292.

Douglas, B. C., M. S. Kearney, and S. P. Leatherman (eds.): 2001, *Sea Level Rise: History and Consequences*. San Diego: Academic Press.

Douglas, B. C. and W. R. Peltier: 2002, 'The Puzzle of Global Sea-Level Rise'. *Physics Today* **55**, 35–40.

Ekman, M.: 1996, 'A Consistent Map of the Postglacial Uplift of Fennoscandia'. *Terra Nova* **8**, 158–165.

Emery, K. O. and D. G. Aubrey: 1991, *Sea Levels, Land Levels, and Tide Gauges*. New York: Springer.

Fairbridge, R. W. and C. Hillaire-Marcel: 1977, 'An 8,000-yr Palaeoclimatic Record of the 'Double-Hale' 45-yr Solar Cycle'. *Nature* **268**, 413–416.

Fang, M. and B. F. Hager: 2002, 'On the Apparent Exponential Relaxation Curves at the Central Regions of the Last Pleistocene Ice Sheets'. In: J. X. Mitrovica and B. L. A. Vermeersen (eds.): *Ice Sheets, Sea Level, and the Dynamic Earth*. Washington: American Geophysical Union, pp. 201–218.

Farrand, W. R.: 1962, 'Postglacial Uplift in North America'. *American Journal of Science* **260**, 181–199.

Farrand, W. R. and R. T. Gajda: 1962, 'Isobases of the Wisconsin Marine Limit in Canada'. *Geographical Bulletin Ottawa* **17**, 5–22.

Forte, A. M. and J. X. Mitrovica: 1996, 'New Inferences of Mantle Viscosity from Joint Inversion of Long-Wavelength Mantle Convection and Post-Glacial Rebound Data'. *Geophysical Research Letters* **23**, 1147–1150.

Gendt, G., G. Dick, W. Mai, T. Nischan, and W. Sommerfeld: 1994, *Nutzerhandbuch zum Programmsystem EPOS.P.V2 (Earth Parameters and Orbit Determination System) für die Analyse von GPS-Daten*. Potsdam: GeoForschungsZentrum Potsdam.

Gough, W. A. and C. A. Robinson: 2000, 'Sea-level Variation in Hudson Bay, Canada, from Tide-Gauge Data'. *Arctic, Antarctic and Alpine Research* **32**, 331–335.

Gutenberg, B.: 1941, 'Changes in Sea Level, Postglacial Uplift, and the Mobility of the Earth's Interior'. *Geological Society of America Bulletin* **52**, 721–772.

Gutenberg, B.: 1942, 'Is the Land around Hudson Bay at Present Rising?'. *American Journal of Science* **240**, 147–149.

Gutenberg, B.: 1954, 'Postglacial Uplift in the Great Lakes Region'. *Archives for Meteorology, Geophysics and Bioclimatology, Series A* **7**, 243–251.

Gutenberg, B.: 1958, 'Rheological Problems of the Earth's Interior'. In: F. R. Eirich (ed.): *Rheology: Theory and Applications, Vol. 2*. New York: Academic Press, pp. 401–431.

Hagedoorn, J. M.: 2005, *Glaziale Isostasie und Rezente Meeresspiegeländerung*, Dissertation. Stuttgart: University of Stuttgart.

Hagedoorn, J. M. and D. Wolf: 2003, 'Pleistocene and Recent Deglaciation in Svalbard: Implications for Tide-Gauge, GPS and VLBI Measurements'. *Journal of Geodynamics* **35**, 415–423.

Han, D. and J. Wahr: 1995, 'The Viscoelastic Relaxation of a Realistically Stratified Earth, and a Further Analysis of Postglacial Rebound'. *Geophysical Journal International* **120**, 287–311.

Hansell, R. I. C., P. A. Scott, R. Staniforth, and J. Svoboda: 1983, 'Permafrost Development in the Intertidal Zone at Churchill, Manitoba: A Possible Mechanism for Accelerated Beach Uplift'. *Arctic* **36**, 198–203.

Hillaire-Marcel, C. and R. W. Fairbridge: 1978, 'Isostasy and Eustasy of Hudson Bay'. *Geology* **6**, 117–122.

Hubbard, B. B.: 1997, *Wavelets, die Mathematik der kleinen Wellen*. Basel: Birkhäuser Verlag.

Innes, M. J. S.: 1948, 'Gravity Anomalies in Northwestern Canada'. *Canadian Journal of Research* **26A**, 199–203.

Jeffreys, H.: 1952, *The Earth: Its Origin, History and Physical Constitution*. Cambridge: Cambridge University Press, 3rd edition.

Jeffreys, H.: 1976, *The Earth: Its Origin, History and Physical Constitution*. Cambridge: Cambridge University Press, 6th edition.

Johnston, W. G.: 1939, 'Recent Changes of Level of the Land Relative to Sea Level'. *American Journal of Science* **237**, 94–98.

Lambeck, K.: 1980, *The Earth's Variable Rotation: Geophysical Causes and Consequences*. Cambridge: Cambridge University Press.

Lambeck, K., C. Smither, and M. Ekman: 1998, 'Tests of Glacial Rebound Models for Fennoscandinavia Based on Instrumented Sea- and Lake-Level Records'. *Geophysical Journal International* **135**, 375–387.

Lambert, A., N. Courtier, G. S. Sagawa, F. Klopping, D. Winester, T. M. James, and J. O. Liard: 2001, 'New Constraints on Laurentide Postglacial Rebound from Absolute Gravity Measurements'. *Geophysical Research Letters* **28**, 2109–2112.

Lambert, A., T. S. James, J. O. Liard, and N. Courtier: 1996, 'The Role and Capability of Absolute Gravity Measurement in Determining the Temporal Variations in the Earth's Gravity Field'. In: R. H. Rapp, A. A. Cazenave, and R. S. Nerem (eds.): *Global Gravity Field and its Temporal Variations*. Berlin: Springer, pp. 20–29.

Lambert, A., T. S. James, and L. H. Thorleifson: 1998, 'Combining Geomorphological and Geodetic Data to Determine Postglacial Tilting in Manitoba'. *Journal of Paleolimnology* **19**, 365–376.

Lambert, A., J. O. Liard, N. Courtier, and D. R. Bower: 1994, 'Absolute Gravimetry Applied to Postglacial Rebound Studies: Progress in Laurentia'. In: B. E. Schutz, A. Anderson, C. Froidevaux, and M. Parke (eds.): *Gravimetry and Space Techniques Applied to Geodynamics and Ocean Dynamics*. Washington: American Geophysical Union, pp. 1–7.

Lambert, A., J. O. Liard, N. Courtier, A. K. Goodacre, and R. K. McConnell: 1989, 'Canadian Absolute Gravity Program: Applications in Geodesy and Geodynamics'. *EOS, Transactions, American Geophysical Union* **70**, 1447, 1459, 1460.

Larson, K. M. and T. van Dam: 2000, 'Measuring Postglacial Rebound with GPS and Absolute Gravity'. *Geophysical Research Letters* **27**, 3925–3928.

Lisitzin, E.: 1974, *Sea-Level Changes*. Amsterdam: Elsevier.

Manning, T. H.: 1951, 'Remarks on the Tides and Driftwood Strand Lines Along the East Coast of James Bay'. *Arctic* **4**, 122–130.

Martinec, Z.: 2000, 'Spectral–Finite Element Approach for Three-Dimensional Viscoelastic Relaxation in a Spherical Earth'. *Geophysical Journal International* **142**, 117–141.

Meier, M. F. and J. M. Wahr: 2002, 'Sea Level is Rising: Do We Know Why?'. *Proceedings of the National Academy of Sciences of the United States of America* **99**, 6524–6526.

Mitrovica, J. X.: 1996, 'Haskell [1935] Revisited'. *Journal of Geophysical Research, Solid Earth* **94**, 555–569.

Mitrovica, J. X.: 1997, 'Going Halves Over the Hudson Bay'. *Nature* **390**, 444–446.

Mitrovica, J. X. and A. M. Forte: 2002, 'On the Radial Profile of Mantle Viscosity'. In: J. X. Mitrovica and B. L. A. Vermeersen (eds.): *Ice Sheets, Sea Level and the Dynamic Earth*. Washington: American Geophysical Union, pp. 187–200.

Mitrovica, J. X. and A. M. Forte: 2004, 'A New Inference of Mantle Viscosity Based upon Joint Inversion of Convection and Glacial Isostatic Adjustment Data'. *Earth and Planetary Science Letters* **225**, 177–189.

Mitrovica, J. X., A. M. Forte, and M. Simons: 2000, 'A Reappraisal of Postglacial Decay Times from Richmond Gulf and James Bay, Canada'. *Geophysical Journal International* **142**, 783–800.

Mitrovica, J. X. and W. R. Peltier: 1992, 'Constraints on Mantle Viscosity from Relative Sea Level Variations in Hudson Bay'. *Geophysical Research Letters* **19**, 1185–1188.

Mitrovica, J. X. and W. R. Peltier: 1993, 'A New Formalism for Inferring Mantle Viscosity Based on Estimates of Post Glacial Decay Times: Application to RSL Variations in N.E. Hudson Bay'. *Geophysical Research Letters* **20**, 2183–2186.

Mitrovica, J. X. and W. R. Peltier: 1995, 'Constraints on Mantle Viscosity Based upon the Inversion of Post-Glacial Uplift Data from the Hudson Bay Region'. *Geophysical Journal International* **122**, 353–377.

Moore, S.: 1948, 'Crustal Movement in the Great Lakes Area'. *Geological Society of America Bulletin* **59**, 697–710.

Nakada, M.: 1983, 'Rheological Structure of the Earth's Mantle Derived from Glacial Rebound in Laurentide'. *Journal of Physics of the Earth* **31**, 349–386.

Nakada, M. and K. Lambeck: 1991, 'Late Pleistocene and Holocene Sea-Level Change; Evidence for Lateral Mantle Viscosity Structure?'. In: R. Sabadini, K. Lambeck, and E. Boschi (eds.): *Glacial Isostasy, Sea Level and Mantle Rheology.* Dordrecht: Kluwer, pp. 79–94.

Park, K.-D., R. S. Nerem, J. L. Davis, M. S. Schenewerk, G. A. Milne, and J. X. Mitrovica: 2002, 'Investigation of Glacial Isostatic Adjustment in the Northeast U.S. Using GPS Measurements'. *Geophysical Research Letters* **29**, doi:10.1029/2001GL013782.

Peltier, W. R.: 1994, 'Ice Age Paleotopography'. *Science* **265**, 195–201.

Peltier, W. R.: 1996, 'Mantle Viscosity and Ice-Age Ice Sheet Topography'. *Science* **273**, 1359–1364.

Peltier, W. R.: 1998, 'Postglacial Variations in the Level of the Sea: Implications for Climate Dynamics and Solid-Earth Geophysics'. *Reviews of Geophysics* **36**, 603–689.

Peltier, W. R.: 1999, 'Global Sea Level Rise and Glacial Isostatic Adjustment'. *Global and Planetary Change* **20**, 93–123.

Peltier, W. R.: 2004, 'Global Glacial Isostasy and the Surface of the Ice-Age Earth: The ICE5G (VM2) Model and GRACE'. *Annual Review of Earth and Planetary Sciences* **32**, 111–149.

Peltier, W. R. and J. T. Andrews: 1983, 'Glacial Geology and Glacial Isostasy of the Hudson Bay Region'. In: D. E. Smith and A. G. Dawson (eds.): *Shorelines and Isostasy.* London: Academic Press, pp. 285–319.

Plag, H.-P.: 1988, *A Regional Study of Norwegian Coastal Long-Period Sea-Level Variations and their Causes*, Berliner Geowissenschaftliche Abhandlungen, Reihe B Nr. 4. Berlin: Dietrich Reimer Verlag.

Rabbel, W. and J. Zschau: 1985, 'Static Deformations and Gravity Changes at the Earth's Surface due to Atmospheric Loading'. *J. Geophys.* **56**, 81–99.

Sabadini, R. and B. Vermeersen: 2004, *Global Dynamics of the Earth—Applications of Normal Mode Relaxation Theory to Solid-Earth Geophysics.* Dordrecht: Kluwer Academic Publishers.

Scherneck, H.-G., J. M. Johansson, G. Elgered, J. L. Davis, B. Jonsson, G. Hedling, H. Koivula, M. Ollikainen, M. Poutanen, M. Vermeer, J. X. Mitrovica, and

G. A. Milne: 2002, 'BIFROST: Observing the Three-Dimensional Deformation of Fennoscandia'. In: J. X. Mitrovica and L. L. A. Vermeersen (eds.): *Ice Sheets, Sea Level and the Dynamic Earth.* Washington: American Geophysical Union, pp. 69–93.

Simons, M. and B. H. Hager: 1997, 'Localization of the Gravity Field and the Signature of Glacial Rebound'. *Nature* **390**, 500–504.

Stanley, G. M.: 1939, 'Raised Beaches on the East Coast of James and Hudson Bays (Abstract)'. *Geological Society of America Bulletin* **50**, 1936–1937.

Stuiver, M. and P. J. Reimer: 1993, 'Extended ^{14}C Data Base and Revised CALIB 3.0 ^{14}C Age Calibration Program'. *Radiocarbon* **35**, 215–230.

Torrence, C. and G. P. Compo: 1998, 'A Practical Guide to Wavelet Analysis'. *Bulletin of the American Meteorological Society* **79**, 61–78.

Tushingham, A. M.: 1992, 'Observations of Postglacial Uplift at Churchill, Manitoba'. *Canadian Journal of Earth Science* **29**, 2418–2425.

Tushingham, A. M. and W. R. Peltier: 1991, 'Ice-3G: A New Global Model of the Late Pleistocene Deglaciation Based upon Geophysical Predictions of Post-Glacial Relative Sea Level Change'. *Journal of Geophysical Research, Solid Earth* **96**, 4497–4523.

Tyrrell, J. B.: 1894, 'Notes on the Pleistocene of the North-West Territories of Canada, North-West and West of Hudson Bay'. *Geological Magazine* **1**, 395–399.

Tyrrell, J. B.: 1896, 'Is the Land around Hudson Bay at Present Rising?'. *American Journal of Science, Series 4* **2**, 200–205.

van Dam, T. M., G. Blewitt, and M. B. Heflin: 1994, 'Atmospheric Pressure Loading Effects on Global Positioning System Coordinate Determinations'. *Journal of Geophysical Research, Solid Earth* **99**, 23939–23950.

van Dam, T. M., J. Wahr, P. C. D. Milly, A. B. Sihmakin, G. Blewitt, D. Lavallée, and K. M. Larson: 2001, 'Crustal Displacements due to Continental Water Loading'. *Geophysical Research Letters* **28**, 651–654.

van Dam, T. M. and J. M. Wahr: 1987, 'Displacement of the Earth's Surface due to Atmospheric Loading: Effects on Gravity and Baseline Measurements'. *Journal of Geophysical Research, Solid Earth* **92**, 1281–1286.

Vaníček, P. and D. Nagy: 1979, *Report on the Compilation of the Map of Recent Crustal Movements in Canada*, Department of Surveying Engineering, Technical Report No. 66. Fredericton: University of New Brunswick.

Virtanen, H.: 2004, 'Loading Effects in Metsähovi from the Atmosphere and the Baltic Sea'. *Journal of Geodynamics* **38**, 407–422.

Walcott, R. I.: 1972, 'Late Quaternary Vertical Movements in Eastern North America: Quantitative Evidence of Glacio-Isostatic Rebound'. *Reviews of Geophysics and Space Physics* **10**, 849–884.

Walcott, R. I.: 1980, 'Rheological Models and Observational Data of Glacio-Isostatic Rebound'. In: N.-A. Mörner (ed.): *Earth Rheology, Isostasy, and Eustasy*. Chichester: J. Wiley, pp. 3–10.

Wessel, P. and W. H. F. Smith: 1991, 'Free Software Helps Map and Display Data'. *EOS, Transactions, American Geophysical Union* **72**, 441–446.

Wolf, D.: 1993, 'The Changing Role of the Lithosphere in Models of Glacial Isostasy: A Historical Review'. *Global and Planetary Change* **8**, 95–106.

Wolf, D., J. Hagedoorn, and Z. Martinec: 2002, 'A new Time-Domain Method of Implementing the Sea-Level Equation in Glacial-Isostatic Adjustment'. *EOS, Transactions, American Geophysical Union* **83** (Fall Meeting Supplement), G12A–1059.

Zhang, F. P. and D. Dong: 2002, 'Seasonal Vertical Crustal Motions in China Detected by GPS'. *Chinese Science Bulletin* **47**, 1772–1779.

Zhang, J.: 1996, *Continuous GPS Measurements of Crustal Deformation in Southern California*, Ph. D. thesis. San Diego: University of California.

Appendix

A. Mathematical symbols

LATIN SYMBOLS

Symbol	*Name*
a	intercept
c	scaling term
$\mathcal{D}_1$, $\mathcal{D}_2$	depth intervals

$g^{(0)}$	unperturbed gravity
$g^{(\Delta)}$	local incremental gravity
$\bar{\dot{g}}_{\mathrm{com}}$	computational mean rate of gravity change
$\bar{\dot{g}}_{\mathrm{obs}}$	observational mean rate of gravity change
h_{L}	lithosphere thickness
N	total number of monthly values considered
P	total number of SLIs considered
(r_X, r_Y, r_Z)	rotation angles
s	RSL height
s_{com}	computational RSL height
s_{obs}	observational RSL height
$s_{\mathrm{obs}}^{\mathrm{max}}$	upper bound on observational RSL height
$s_{\mathrm{obs}}^{\mathrm{min}}$	lower bound on observational RSL height
Δs	width of linear ramps of membership function
s_{LR}	RSL height based on linear regression
s_n	monthly RSL height for nth month
$\bar{\dot{s}}_{\mathrm{com}}$	computational mean rate of RSL change
$\bar{\dot{s}}_{\mathrm{obs}}$	observational mean rate of RSL change
t	time epoch
t_{cal}	calibrated age
$t_{\mathrm{cal}}^{\mathrm{max}}$	upper bound on calibrated age
$t_{\mathrm{cal}}^{\mathrm{min}}$	lower bound on calibrated age
t_{C14}	^{14}C age
t_n	reference time epoch for s_n
(t_X, t_Y, t_Z)	translation components
$(u_r, u_\lambda, u_\varphi)$	radial, longitudinal and latitudinal displacement components
$\bar{\dot{u}}_{\mathrm{com}}$	computational mean rate of topographic-height change
$\bar{\dot{u}}_{\mathrm{obs}}$	observational mean rate of topographic-height change
w	membership function

w_p	membership function for pth SLI
(X, Y, Z)	daily position coordinates
$(\overline{X}, \overline{Y}, \overline{Z})$	mean position coordinates
$(\Delta X, \Delta Y, \Delta Z)$	residual position coordinates
$(\Delta E, \Delta N, \Delta H)$	east, north and topographic-height coordinates

Greek symbols

Symbol	*Name*
ϵ	standard error of $\bar{\dot{g}}_{\rm obs}$, $\bar{\dot{s}}_{\rm obs}$ or $\bar{\dot{u}}_{\rm obs}$
$\epsilon_{\rm cal}$	standard error of calibrated age
$\epsilon_{\rm C14}$	standard error of ^{14}C age
$\eta_{\rm LM}$	lower-mantle viscosity
$\eta_{\rm UM}$	upper-mantle viscosity
λ	longitude of station or SLI
σ	standard deviation
$\phi^{(\Delta)}$	local incremental gravitational potential
φ	latitude of station or SLI
$\chi(\bar{\dot{f}})$	misfit function for $\bar{\dot{f}}$
$\chi(s)$	misfit function for RSL height

B. Abbreviations

Abbreviation	*Name*
BADC	British Atmospheric Data Centre
BMBF	Bundesministerium für Bildung und Forschung (Germany)
CH	Churchill
CHS	Canadian Hydrographic Service

CHUR	GPS station Churchill
EC	east coast of North America
EPOS	Earth Parameters and Orbit Determination System
GFZ	GeoForschungsZentrum Potsdam (Germany)
GIA	glacial-isostatic adjustment
GMSLP2.1f	Global Mean Sea-Level Pressure v.2.1f
GSC	Geological Survey of Canada
GSD	Geodetic Survey Division (Canada)
HM	Cape Henrietta Maria
IB	inverse barometer
IGS	International GPS Service
ITRF	International Terrestrial Reference Frame
JB	James Bay
KW	Keewatin
LCRF	loosely constrained reference frame
MEDS	Marine Environmental Data Service (Canada)
MJD	modified Julian day
MSB	Marine Science Branch (Canada)
NGS	National Geodetic Survey (USA)
NOAA	National Oceanic and Atmospheric Administration (USA)
OI	Ottawa Islands
PSMSL	Permanent Service for Mean Sea Level
RG	Richmond Gulf
RLR	revised local reference
RSL	relative sea level
SE	south-east Hudson Bay
SEAL	Sea Level: An Integrated Approach to its Quantification
SI	Southampton Island
SLI	sea-level indicator

UP Ungava Peninsula

List of Figures

List of Tables

V Characteristics of SLIs for region CH. For each sample are given laboratory dating number, Lab. No., SLI type (B: bone, C: charcoal, P: peat, S: shell, W: wood), longitude, λ, latitude, φ, RSL-height range, $s_{\rm obs}^{\rm min}$, $s_{\rm obs}^{\rm max}$, reservoir-corrected ^{14}C age, $t_{\rm C14}$, its standard error, $\epsilon_{\rm C14}$ and 2σ-calibrated age range, $t_{\rm cal}^{\rm min}$, $t_{\rm cal}^{\rm max}$. If $s_{\rm obs}^{\rm min}$ or $s_{\rm obs}^{\rm max}$ is not given, the sample represents an upper or lower bound on RSL height, respectively. If both $s_{\rm obs}^{\rm min}$ and $s_{\rm obs}^{\rm max}$ are given, the sample represents a finite range for RSL height. Ages are measured with respect to present time (AD 1950). 72

VI Estimates of mantle viscosity, η_1, η_2, for specified depth intervals, $\mathcal{D}_1$, $\mathcal{D}_2$, respectively, based on SLIs from the Hudson Bay region. If $\mathcal{D}_1$ extends to the surface, a lithosphere may be included. The SLIs considered have been grouped according to RSL diagrams for regions CH, HM, JB, KW, OI, RG, SI and UP supplemented by region EC (Figure 7 and Appendix B). The additional consideration of the free-air gravity anomaly over Hudson Bay is indicated by $*$, that of convection-related global data by † and that of RSL data from Fennoscandia by §. Results based on formal inversions are denoted by ¶. 73

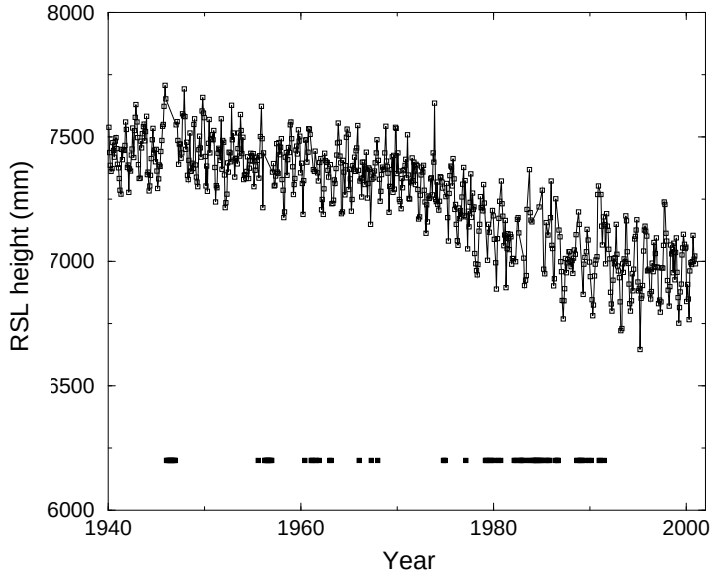

Figure 1. Monthly RSL height at Churchill according to PSMSL data. The horizontal bars indicate data gaps.

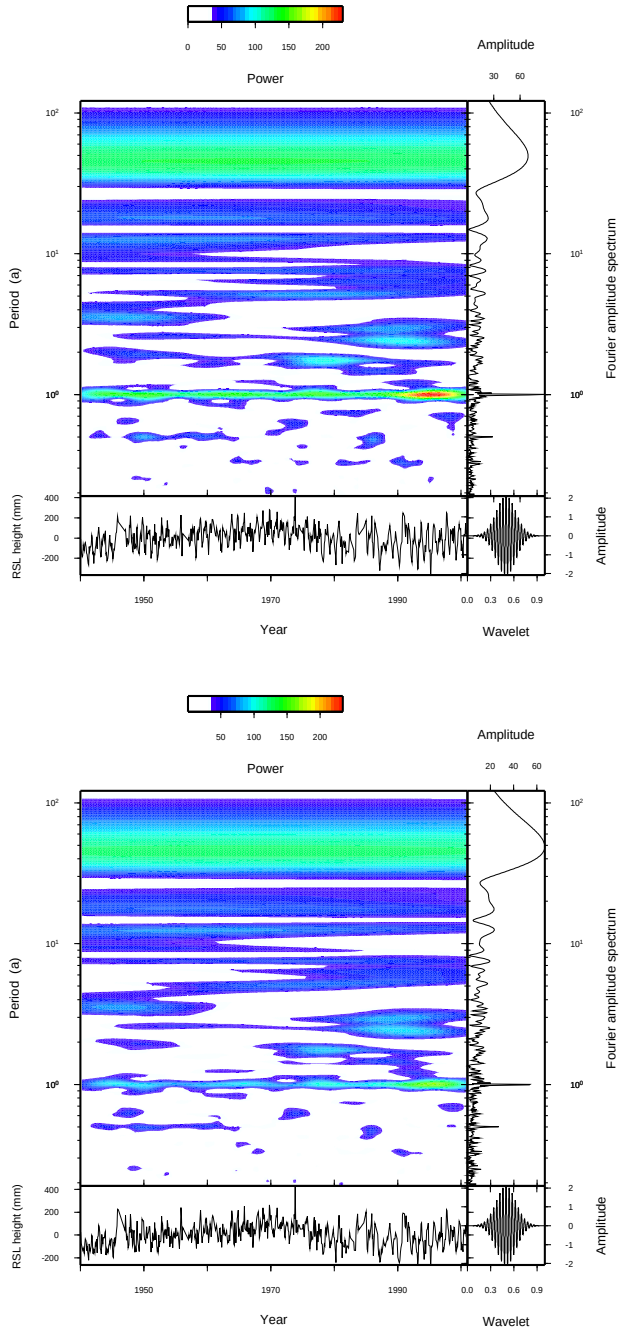

Figure 2. Continuous wavelet transform of monthly RSL height at Churchill according to PSMSL data without (top) and with (bottom) IB reduction. The panels show the wavelet scalogram (upper left), the Fourier amplitude spectrum (upper right), the detrended PSMSL time series (lower left) and the analysing Morlet wavelet (lower right).

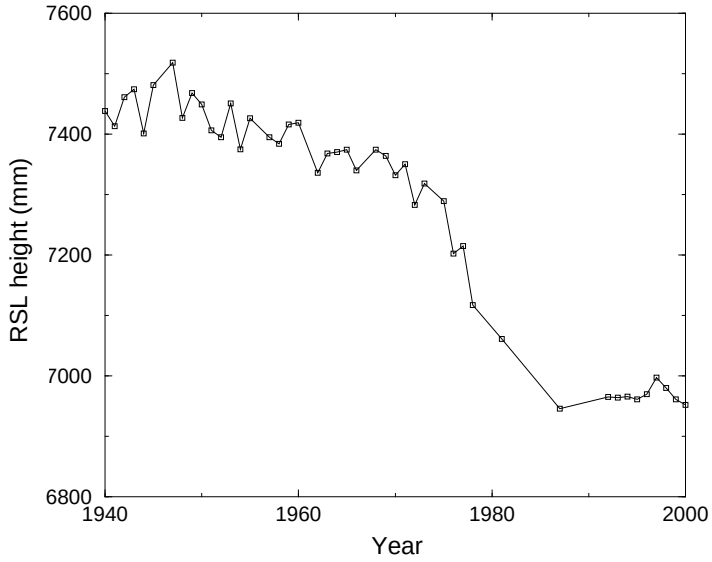

Figure 3. Annual RSL height at Churchill calculated from PSMSL data.

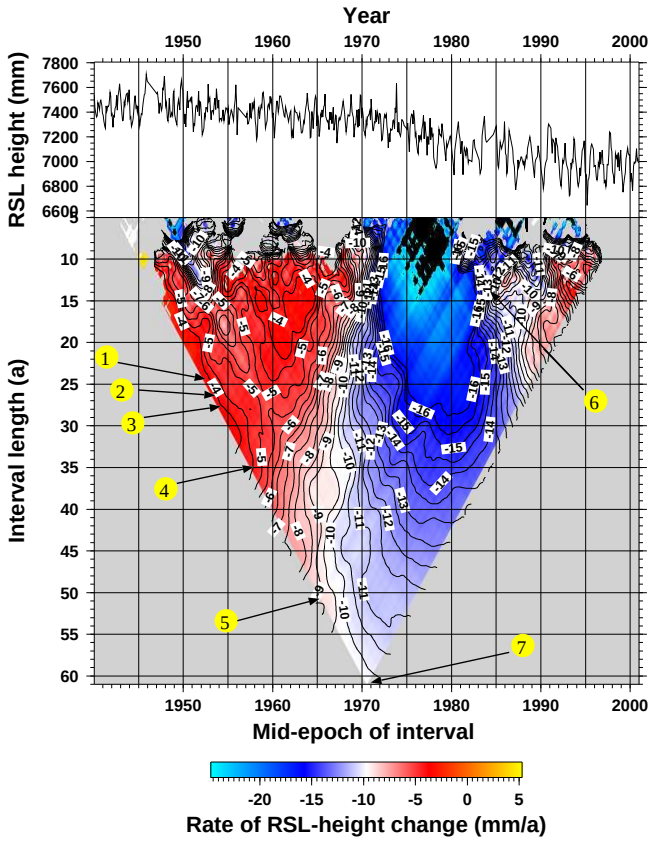

Figure 4. Linear-trend analysis diagram for monthly RSL height at Churchill according to PSMSL data. The panels show the original PSMSL time series (top) and the contour plot of the mean rate of RSL change in mm/a as a function of length and mid-epoch of the observation interval considered (bottom). Grey regions inside the triangle indicate that the hypothesis of a linear trend is refused. Arrows point to previous estimates according to (1) Barnett (1966) for 1940–1964, (2) Dohler and Ku (1970) for 1940–1967, (3) Barnett (1970) for 1940–1968, (4) Vaníček and Nagy (1979) for 1940–1975, (5) Tushingham (1992) for 1940–1991, (6) Tushingham (1992) for 1977–1991 and (7) this study for 1940–2001.

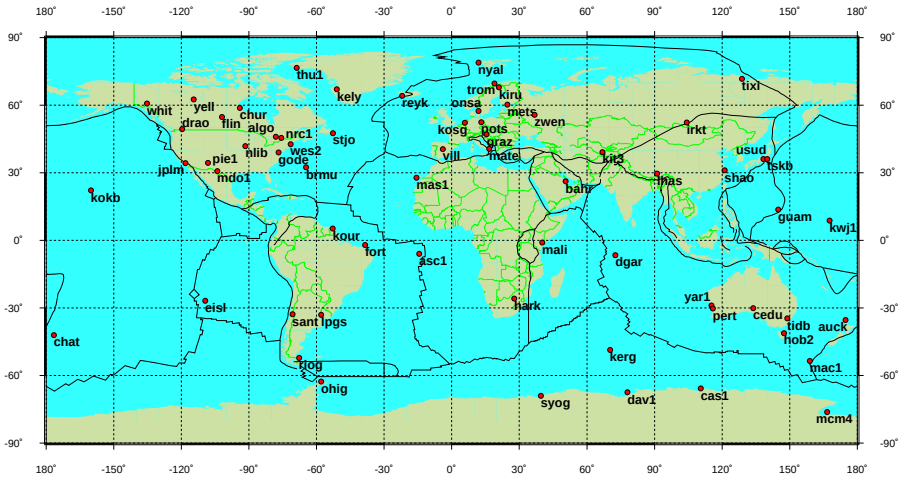

Figure 5. Locations of core GPS stations used for estimating parameters of Helmert transformation.

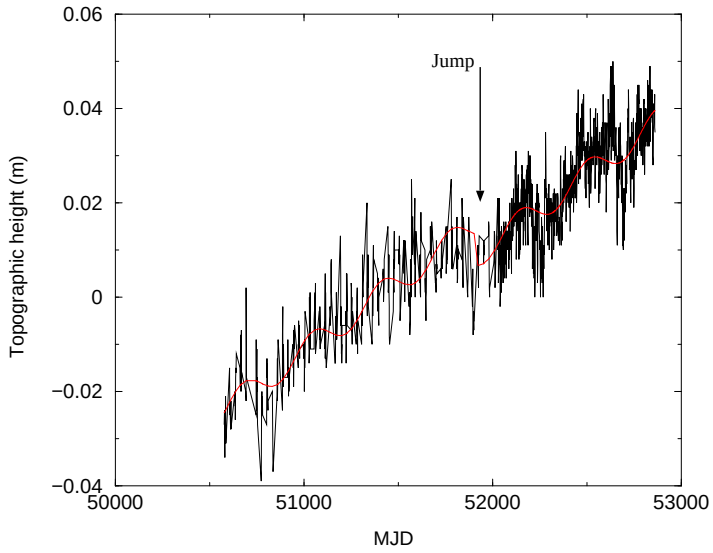

Figure 6. Topographic height at Churchill according to GPS data. The annual wave (red curve) and the jump (arrow) are indicated.

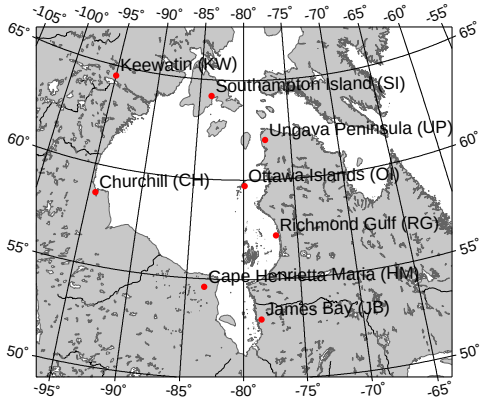

Figure 7. Map of SLI regions considered. Red circles denote the mean locations for the groups of SLIs. The abbreviations of the region names are given in brackets.

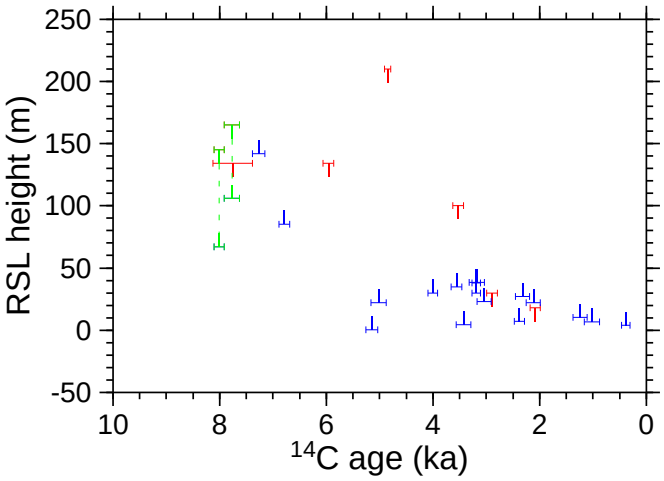

Figure 8. RSL diagram for region CH. SLIs are classified according to whether they provide upper bounds (red), lower bounds (blue) or finite ranges (green) for RSL height. Horizontal bars indicate standard errors of ^{14}C age.

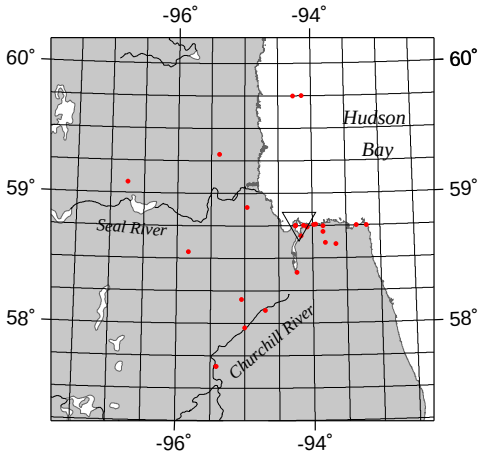

Figure 9. Map of region CH showing locations of SLIs (red dots) as well as tide-gauge and GPS stations (triangle).

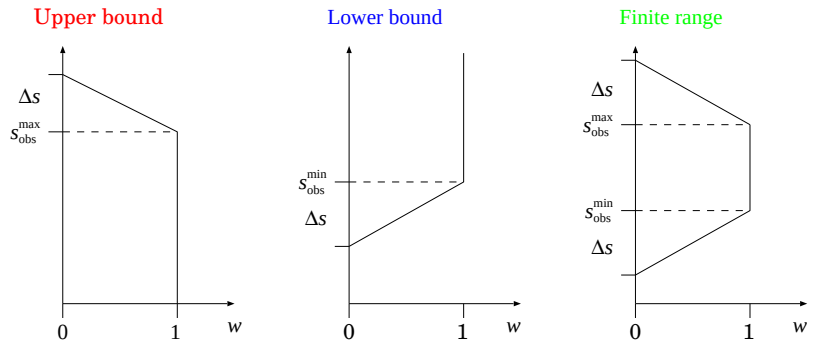

Figure 10. Membership functions, w, used for weighting of fits for RSL height.

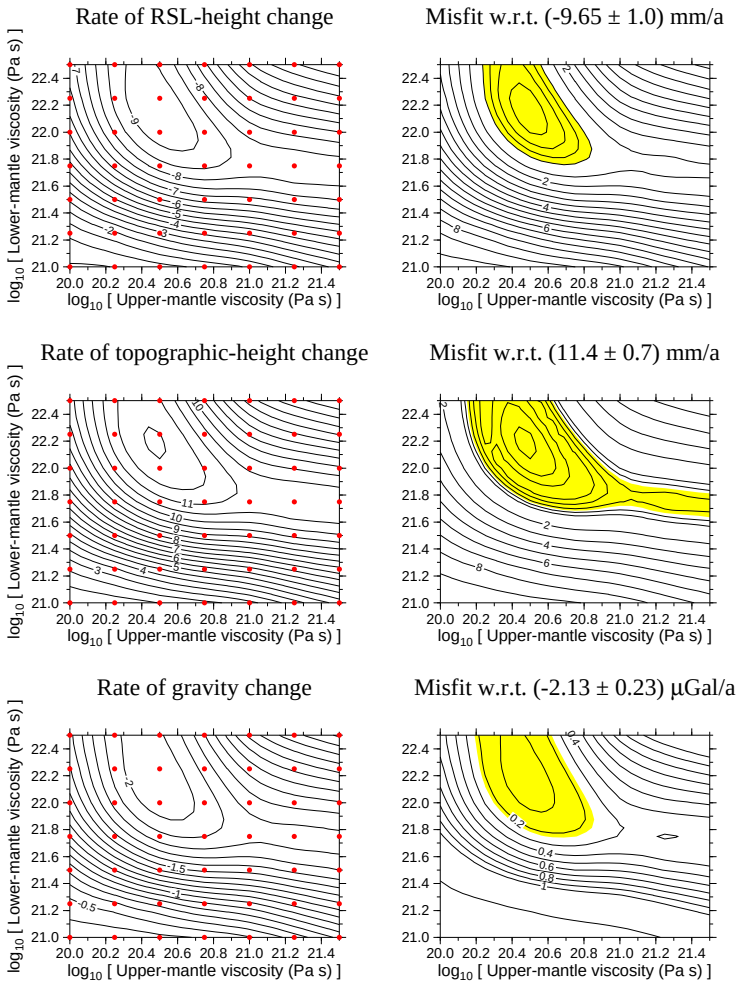

Figure 11. Computational rates of RSL-height change, topographic-height change and gravity change (left) as well as differences to corresponding observational rates (right) as functions of upper- and lower-mantle viscosities. In regions shown in yellow, the differences are smaller than the standard error of the appropriate observational rate.

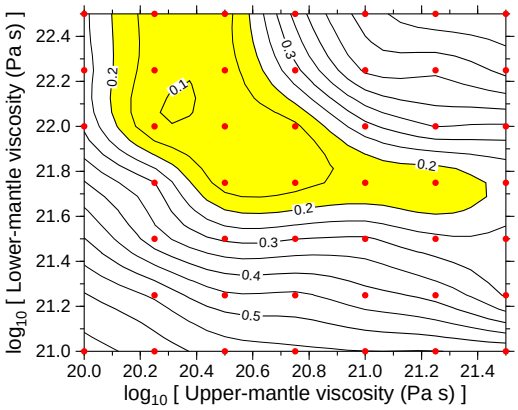

Figure 12. Misfit function for late- and post-glacial RSL height as function of upper- and lower-mantle viscosities. In regions shown in yellow, the misfit is smaller than 0.2.

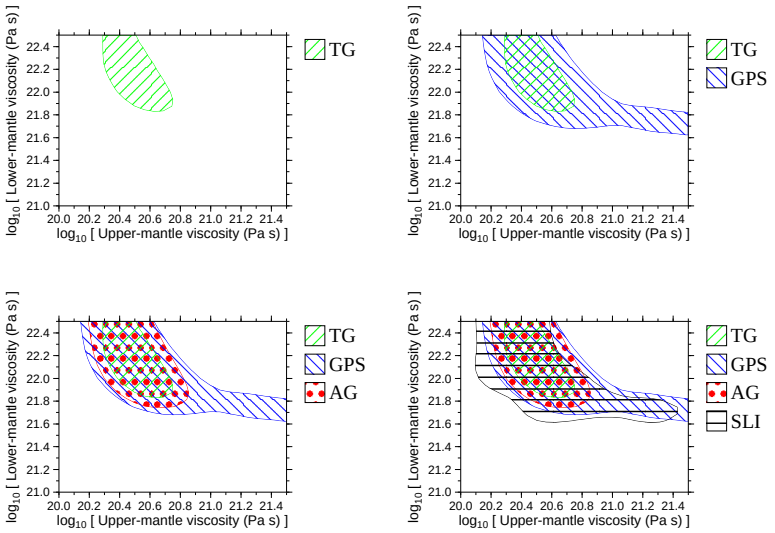

Figure 13. Best fits for rates of RSL-height change (TG), topographic-height change (GPS) and gravity change (AG) and for late- and post-glacial RSL height (SLI) as functions of upper- and lower-mantle viscosities. The individual regions correspond to the yellow regions in Figures 11 and 12.

Table I. Previous estimates of observational mean rate of RSL-height change, $\bar{\dot{s}}_{\rm obs}$, their standard error, ϵ, and standard deviation, σ, based on monthly RSL heights for Churchill and linear regression. The original data were provided by CHS (Gutenberg, 1941; 1942; 1954), MEDS and MSB (Barnett, 1966; 1970). The rate of Gutenberg (1941) is the mean of his separate rates for the months June–November, the rates of Gutenberg (1942) apply to the months June–November (first line) and August–October (second line), the rate of Gutenberg (1954) is based on the months July–September, the other rates were calculated from all monthly RSL heights available. The rate of Barnett (1966) was corrected by Barnett (1970).

Author(s)	Obs. interval	$\bar{\dot{s}}_{\rm obs}$ (mm/a)	ϵ (mm/a)	σ (mm)
Gutenberg (1941)	1928–1939	−29.0	–	–
Gutenberg (1942)	1928–1940	−25.0	7.5	–
	1928–1940	−22.5	7.5	–
Gutenberg (1954)	1929–1951	−10.5	1.8	–
Barnett (1966)	1940–1964	−4.1	–	–
Dohler and Ku (1970)	1940–1967	−3.9	0.7	–
Barnett (1970)	1940–1968	−3.9	–	–
Vaníček and Nagy (1979)	1940–1975	−4.5	0.3	–
Tushingham (1992)	1940–1991	−8.8	0.3	113
Tushingham (1992)	1940–1975	−4.4	0.5	94
Tushingham (1992)	1977–1991	−8.8	2.4	123

Table II. Revised estimates of observational mean rate of RSL-height change, $\bar{\dot{s}}_{\rm obs}$, their standard error, ϵ, and standard deviation, σ, based on N monthly RSL heights for Churchill (PSMSL No. 970141, 58.78°N, 94.20°W) and linear regression. The original RSL heights were provided by PSMSL. The IB reduction implied for the last line is based on GMSLP2.1f air-pressure data provided by BADC.

Obs. interval	N	$\bar{\dot{s}}_{\rm obs}$ (mm/a)	ϵ (mm/a)	σ (mm)
1940–2001	642	−9.72	0.26	116
1940–1975	394	−4.44	0.45	94
1975–2001	260	−10.41	0.95	121
1940–1994	551	−9.43	0.32	115
1940–1994 (IB)	551	−9.65	0.28	102

Table III. Estimates of observational mean rates of (a) topographic-height change, $\bar{\dot{u}}_{\rm obs}$, and (b) gravity change, $\bar{\dot{g}}_{\rm obs}$, their standard error, ϵ, and standard deviation, σ, based on GPS and absolute-gravimetry data for Churchill. The original data were provided by GSC (Lambert et al., 1994; 1996; 1998; 2001), GSD (Larson and van Dam, 2000; Lambert et al., 2001), IGS (Larson and van Dam, 2000; Park et al., 2002; this study), NGS (Lambert et al., 1994) and NOAA (Lambert et al., 1996; 1998; 2001; Larson and van Dam, 2000). The rates of Larson and van Dam (2000) are estimated from their Figure 4.

a)

Author(s)	Obs. interval	$\bar{\dot{u}}_{\rm obs}$ (mm/a)	ϵ (mm/a)	σ (mm)
Larson and van Dam (2000)	1996–2000	10.7	0.23	–
Park et al. (2002)	1995–1999	13.0	0.33	–
This study	1996–2003	11.4	0.70	–

b)

Author(s)	Obs. interval	$\bar{\dot{g}}_{\rm obs}$ (μGal/a)	ϵ (μGal/a)	σ (μGal)
Lambert et al. (1994)	1987–1991	−1.60	–	2.0
Lambert et al. (1996)	1987–1995	−1.45	0.19	1.6
Lambert et al. (1998)	1987–1995	−1.63	0.17	–
Larson and van Dam (2000)	1993–1999	−1.54	0.48	–
Lambert et al. (2001)	1987–1999	−2.13	0.23	–

Table IV. Estimates of relaxation time for the Hudson Bay region according to Walcott (1980) (W80), Mitrovica and Peltier (1993) (MP93), Mitrovica and Peltier (1995) (MP95), Peltier (1996) (P96), Peltier (1998) (P98), Peltier (1999) (P99), Mitrovica et al. (2000) (MFS00) and Fang and Hager (2002) (FH02). The estimates are based on best-fitting exponential functions for RSL diagrams constructed from SLIs grouped into regions CH, HM, JB, KW, OI, RG, SE, SI and UP (Figure 7 and Appendix B).

Author(s)	Relaxation time (ka)								
	CH	HM	JB	KW	OI	RG	SE	SI	UP
W80	–	>5.0	–	–	–	–	–	–	–
MP93	–	–	–	–	2.5	–	–	3.3	2.0
MP95	5.6	17.9	1.5	28.6	2.5	7.6	–	4.9	2.0
P96	5.70	–	3.64	5.73	3.06	7.23	–	4.69	3.34
P98	–	–	3.40	–	–	–	3.43	–	–
P99	–	–	3.26	–	–	4.68	3.90	–	–
MFS00	–	–	2.4	–	–	5.3	–	–	–
FH02	–	–	–	–	–	6.3	–	–	–

Table V. Characteristics of SLIs for region CH. For each sample are given laboratory dating number, Lab. No., SLI type (B: bone, C: charcoal, P: peat, S: shell, W: wood), longitude, λ, latitude, φ, RSL-height range, $s_{\rm obs}^{\rm min}$, $s_{\rm obs}^{\rm max}$, reservoir-corrected ^{14}C age, $t_{\rm C14}$, its standard error, $\epsilon_{\rm C14}$ and 2σ-calibrated age range, $t_{\rm cal}^{\rm min}$, $t_{\rm cal}^{\rm max}$. If $s_{\rm obs}^{\rm min}$ or $s_{\rm obs}^{\rm max}$ is not given, the sample represents an upper or lower bound on RSL height, respectively. If both $s_{\rm obs}^{\rm min}$ and $s_{\rm obs}^{\rm max}$ are given, the sample represents a finite range for RSL height. Ages are measured with respect to present time (AD 1950).

Lab. No., SLI type	λ (°W)	φ (°N)	$s_{\rm obs}^{\rm min}$ (m)	$s_{\rm obs}^{\rm max}$ (m)	$t_{\rm C14}$ (a)	$\epsilon_{\rm C14}$ (a)	$t_{\rm cal}^{\rm min}$ (a)	$t_{\rm cal}^{\rm max}$ (a)
Gx-1063, S	94.7	58.1	67	145	8010	95	8600	9120
GSC-3348, S	95.417	57.667	–	134	7760	370	7955	9430
GSC-3070, S	95.833	58.55	106	165	7770	140	8325	9000
GSC-92, S	95.05	58.183	142	–	7270	120	7905	8305
GSC-2579, S	95.383	59.3	85	–	6790	100	7460	7815
BGS-980, P	95.417	57.667	–	134	5960	100	6530	7035
BGS-796, S	94.237	58.39	0.3	–	5150	110	5680	6155
GSC-1549, S	94.077	58.74	22	–	5020	140	5455	6065
GSC-2567, P	96.75	59.083	–	210	4850	60	5405	5730
GSC-3851, S	94.967	58.892	30	–	4000	90	4240	4740
S-738, S	94.25	58.75	35	–	3560	105	3590	4125
BGS-793, W	95.0	57.967	–	100	3530	100	3585	4050
GSC-735, S	94.17	58.671	4	–	3430	140	3405	4005
Gx-1065, S	94.275	59.75	38	–	3190	80	3260	3590
Gx-1072, S	93.657	58.607	30	–	3190	80	3260	3590
GSC-685, S	93.811	58.619	38.5	–	3180	140	3060	3690
GSC-261, S	94.081	58.747	23	–	3040	130	2895	3495
S-521, B	94.25	58.75	–	30	2895	100	2830	3260
GSC-4507, S	94.143	59.757	7	–	2380	100	2225	2695
GSC-683, S	93.843	58.703	27	–	2320	130	2095	2690
GSC-723, S	93.981	58.757	22	–	2120	130	1830	2360
I-3973, C	94.25	58.75	–	18	2080	95	1880	2260
GSC-682, S	93.841	58.746	10.5	–	1240	130	930	1355
GSC-684, S	93.95	58.760	6.5	–	1020	140	705	1180
Gx-1073, S	93.35	58.75	4	–	385	80	315	535

Table VI. Estimates of mantle viscosity, η_1, η_2, for specified depth intervals, $\mathcal{D}_1$, $\mathcal{D}_2$, respectively, based on SLIs from the Hudson Bay region. If $\mathcal{D}_1$ extends to the surface, a lithosphere may be included. The SLIs considered have been grouped according to RSL diagrams for regions CH, HM, JB, KW, OI, RG, SI and UP supplemented by region EC (Figure 7 and Appendix B). The additional consideration of the free-air gravity anomaly over Hudson Bay is indicated by $*$, that of convection-related global data by † and that of RSL data from Fennoscandia by §. Results based on formal inversions are denoted by ¶.

Table VI.

Author(s)	$\mathcal{D}_1$ (km)	η_1 (10^{21} Pa s)	$\mathcal{D}_2$ (km)	η_2 (10^{21} Pa s)	SLI region(s)									Remarks
Nakada (1983)	0–200	0.5	200–2900	100	CH	–	–	–	–	–	–	–	–	*
	0–200	0.05–0.75	200–2900	100	CH	HM	–	–	OI	–	SI	–	–	*
Peltier and Andrews (1983)	0–670	1	670–2900	1–3	CH	–	–	–	OI	RG	–	–	EC	*
Nakada and Lambeck (1991)	0–670	0.4–0.6	670–2900	20–50	CH	HM	–	–	OI	–	–	–	–	
Mitrovica and Peltier (1992)	0–670	1	670–2900	1–3	–	–	JB	KW	OI	RG	SI	UP	–	
	670–1800	1	–	–	–	–	JB	KW	OI	RG	SI	UP	–	¶
Mitrovica and Peltier (1993)	500–1870	0.66–1.2	–	–	–	–	–	–	OI	–	SI	UP	–	¶
Han and Wahr (1995)	0–670	0.6–1	670–2900	30–50	CH	HM	–	KW	OI	–	SI	UP	–	*
Mitrovica and Peltier (1995)	0–670	0.5	670–2900	0.5–3	–	HM	JB	–	OI	RG	SI	UP	–	
	500–1870	0.71–1.1	–	–	–	–	JB	–	OI	RG	SI	UP	–	¶
Forte and Mitrovica (1996)	0–1400	0.76	–	–	–	–	–	–	–	RG	–	–	–	† § ¶
	400–1800	1.9	–	–	–	–	–	–	–	RG	–	–	–	† § ¶
Mitrovica (1996)	670–2900	> 2.4	–	–	–	–	–	–	–	RG	–	–	–	
	670–2000	1.4–3.3	–	–	–	–	–	–	–	RG	–	–	–	§ ¶
	670–2000	0.79	–	–	–	–	–	–	OI	–	SI	UP	–	§ ¶
Cianetti et al. (2002)	0–670	1	670–2900	2	CH	HM	JB	KW	OI	RG	SI	UP	–	
	0–670	3.2	670–2900	4.0	CH	–	–	–	–	–	–	–	–	¶
	0–670	0.16	670–2900	2.0	CH	HM	JB	KW	OI	RG	SI	UP	–	¶
Mitrovica and Forte (2002)	0–670	0.39–0.43	670–2900	6.5–11	–	–	JB	–	–	RG	–	–	–	† § ¶
Mitrovica and Forte (2004)	0–670	0.5	670–2900	1.0	–	–	JB	–	–	RG	–	–	–	§ ¶